On Data Compression for TDOA Localization

PATRIK HEDSTRÖM, JOEL ARBRING

FOI, Swedish Defence Research Agency, is a mainly assignment-funded agency under the Ministry of Defence. The core activities are research, method and technology development, as well as studies conducted in the interests of Swedish defence and the safety and security of society. The organisation employs approximately 1000 personnel of whom about 800 are scientists. This makes FOI Sweden's largest research institute. FOI gives its customers access to leading-edge expertise in a large number of fields such as security policy studies, defence and security related analyses, the assessment of various types of threat, systems for control and management of crises, protection against and management of hazardous substances, IT security and the potential offered by new sensors.

FOI
Defence Research Agency
Informations Systems
SE-581 11 Linköping

Phone: +46 13 37 80 00
Fax: +46 13 37 81 00

www.foi.se

FOI-R-- 3024 --SE Scientific report
ISSN 1650-1942 October 2010

Informations Systems

Patrik Hedström, Joel Arbring

On Data Compression for TDOA Localization

Titel	Datakompression för TDOA-lokalisering
Title	On Data Compression for TDOA Localization

Rapportnr/Report no	FOI-R--3024--SE
Rapporttyp Report Type	Vetenskaplig rapport Scientific report
Sidor/Pages	106 p
Månad/Month	Oktober/October
Utgivningsår/Year	2010
ISSN	ISSN 1650-1942
Kund/Customer	Försvarsmakten
Projektnr/Project no	E7130
Godkänd av/Approved by	Magnus Jändel

FOI, Totalförsvarets Forskningsinstitut
Avdelningen för Informationssystem
Box 1165
581 11 Linköping

FOI, Swedish Defence Research Agency
Information Systems
Box 1165
SE-581 11 Linköping

Sammanfattning

Den här exjobbsrapporten undersöker olika tillvägagångssätt för att komprimera vanliga signaltyper i ett TDOA-lokaliseringsystem. Rapporten innehåller även utvärdering av kompressionteknikerna på inspelad data, insamlad som del av exjobbsarbetet. Den utvärderingen visar att det är möjligt att komprimera signalerna med bibehållen lokaliseringsnoggranhet.

Den insamlade datan komplementeras med mer utförliga simuleringar som använder en frirymdsmodell utan fädning. De undersökta signalerna är signaler med platt spektrum, signaler med fasskiftskodning och en enkelt sidbandsmodulerad talsignal. Signaler med låg bandbredd har getts större vikt än signaler med hög bandbredd, då smalbandinga signaler kräver mer data för att få en tillförlitlig lokaliseringsestimat.

De kompressionsmetoder som använts är olika transform-metoder. De transformer som använts är Karhunen-Loéve-transformen och den diskreta Fourier-transformen. Olika tillvägagångsätt för kvantisering undersöks, en av dem är så kallad zonal sampling.

Lokaliseringen är utförd i Fourier-domänen genom att beräkna ett spatiellt effektsspektrum utifrån en korskorreleringsmatris. Simuleringarna är utförda i Matlab med tre noder med en symmetrisk geometri.

Lokaliseringsnoggrannheten jämförs med Craméer-Rao-gränsen för signaler med platt spektrum med hjälp av standardavvikelsen för lokaliseringsfelet från de komprimerade signalerna.

Nyckelord: TDOA, Lokalisering, Datakompression, CRMB, Telekrig

Summary

This master thesis investigates different approaches to data compression on common types of signals in the context of localization by estimating time difference of arrival (TDOA). The thesis includes evaluation of the compression schemes using recorded data, collected as part of the thesis work. This evaluation shows that compression is possible while preserving localization accuracy.

The recorded data is backed up with more extensive simulations using a free space propagation model without attenuation. The signals investigated are flat spectrum signals, signals using phase shift keying and single side band speech signals. Signals with low bandwidth are given precedence over high bandwidth signals, since they require more data in order to get an accurate localization estimate.

The compression methods used are transform based schemes. The transforms utilized are the Karhunen-Loéve transform and the discrete Fourier transform. Different approaches for quantization of the transform components are examined, one of them being zonal sampling.

Localization is performed in the Fourier domain by calculating the steered response power from the cross-spectral density matrix. The simulations are performed in Matlab using three recording nodes in a symmetrical geometry.

The performance of localization accuracy is compared with the Cramér-Rao bound for flat spectrum signals using the standard deviation of the localization error from the compressed signals.

Keywords: TDOA, Localization, Data compression, CRMB, Electronic Warfare

Contents

Acronyms

Notation	Description	Page List
AM	Amplitude modulation	27
CRB	Cramér-Rao bound	7, 13, 17, 19, 20, **20**, 24, 42, 44, 45, 48, 50, 77, 93
CRMB	Cramér-Rao matrix bound	20, **20**
DCT	Discrete cosine transform	30, **30**, 31, 48, 50
DFT	Discrete Fourier transform	7, 31, **31**, 34, 36, 48, 50, 54, 64, 79, 91, 99
FIM	Fisher information matrix	9, 20, **20**, 43
FOI	Swedish Defence Research Agency	74
FSS	Flat spectrum signal	7, 23, 24, **24**, 34, 36, 42, 44, 45, 49, 50, 59, 64, 72, 76, 77, 79, 89, 93, 96, 99
GPS	Global Positioning System	71, 72, 76
KLT	Karhunen-Loéve transform	7, 30, **30**, 31, 42, 47, 50, 54, 81
PCA	Principal component analysis	30
PSK	Phase-shift keying	7, 24, 26, **26**, 39, 50, 54, 59, 64, 71, 72, 77, 79, 91
SNR	Signal to noise ratio	13, 16, 17, 23, **23**, 24, 34, 36, 42, 43, 45, 48, 50, 52, 54–57, 59, 60, 64, 65, 68, 72, 76, 77, 79, 81, 83, 85, 88, 89, 91, 96
SRP	Steered response power	7, 18, **18**, 19, 46, 76, 90, 94
SSB	Single side band	7, 23, 24, 27, **27**, 30, 36, 39, 50, 52, 54, 59, 68, 71, 72, 77, 79, 89, 90, 93, 99
STFT	Short-time Fourier transform	9, 18, **18**, 31, 39
SVD	Singular Value Decomposition	89
TDOA	Time difference of arrival	7, 8, 11, 12, **15**, 16, 17, 19, 20, 23, 24, 29, 34, 39, 76, 89, 90
TFM	Time-frequency masking	**39**, 64, 68, 85, 90
WGN	White Gaussian noise	23, **24**, 36, 50, 71, 76, 89

Symbols

Notation	Description	Page List
$E[\circ]$	Expected value of $\circ$	16
$\mathcal{F}\{\circ\}$	Fourier transform of $\circ$	16
$\circ^*$	Conjugate transpose of $\circ$	18
$\circ^T$	Transpose of $\circ$	20
$\hat{\circ}$	Estimate of $\circ$	15
$\circ_i$	In-phase component of $\circ$	26
$\circ_q$	Quadrature component of $\circ$	26
$\circ * \circ$	Convolution of $\circ$ and $\circ$	16
B	Bandwidth	11
c	Propagation speed (of light)	15
D	Distortion	42
δ	Dirac's delta function	16
Δ	Time difference of arrival	15
$\mathbf{G}$	Sensor array matrix	20
$\mathbf{g}$	Sensor position matrix	20
H	System function	16
h	Impulse response	16
$\mathbf{J}$	The Fisher information matrix (FIM)	20
j	Imaginary unit	16
K	Number of components chosen	34
k	Frequency index	18
κ	Noise coefficient	23
L	Number of blocks	18
l	Block index	18
L_B	Block length	18, 47
M	Number of receivers	11
N	Number of samples	20
ν	Noise	15
ω	Angular frequency	16
P	Signal power	23
p	Receiver	16
$\mathbf{p}$	Receiver position vector	15
q	Transmitter	16
$\mathbf{q}$	Transmitter position vector	15
R_x	The auto-correlation matrix of x	30
R	Data rate, bits per sample	38, 42, 59
$r(\tau)$	Cross correlation function	15
s	Transmitted signal	15
σ	Standard deviation	20, 38
σ^2	Variance	20
$S(\omega)$	Cross spectral density function	16
T	Measured time	20
t	Time	15
θ	Phase offset	26, 77
$\mathbf{u}$	Position vector	18
w	Hamming Window	18
x	Received signal	15

Notation	Description	Page List
χ	x arranged in blocks	30
$X(l,\omega)$	STFT of received signal	18

1 Introduction

In electronic warfare, one objective is localization of transmitters. One way of doing this is by sampling the signal with three or more receivers at different positions and estimating the time difference of arrival (TDOA)[1] of the signal. By doing this it is possible to triangulate the location of the transmitter. A common system setup used for localization is illustrated in figure 1.1 with three receivers and one transmitter.

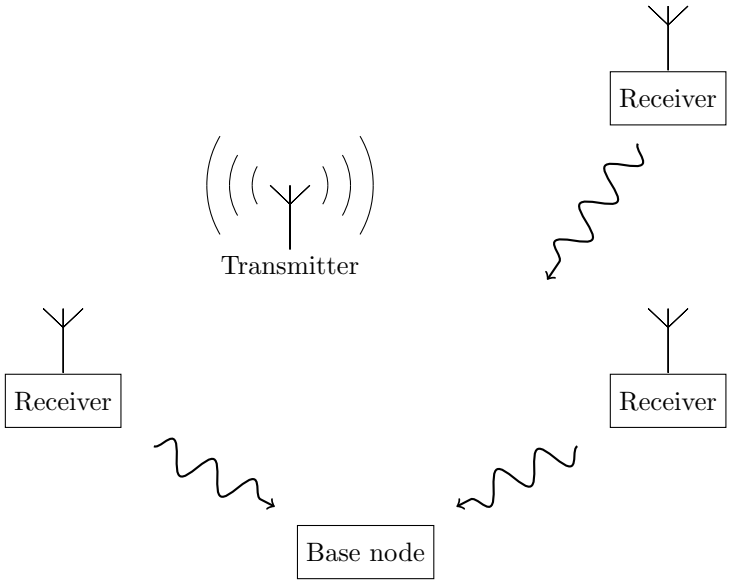

Figure 1.1: A common system setup used for localization in electronic warfare scenarios. Each receiver retransmits the signal to the base node for correlation.

To estimate the TDOA, data must be gathered and correlated from all receivers. One problem is that the channel capacity between the receivers is limited, therefore one may wish to reduce the amount of data needed to be sent for correlation.

Given M receivers and a signal bandwidth of B Hz the bandwidth of the channel needs to be $M \cdot B$ Hz. A simple example can be calculated for 10 MHz instantaneous bandwidth, this gives a receiving data rate of $10^7 \cdot 8 \cdot 2 = 160$ Mbit per second given an 8 bit word length and sampling done at the Nyquist frequency. Table 1.1 on the following page gives the transmission rates of different connections used in localization systems.

This thesis investigates the possibility of data reduction in the application of estimating TDOA. If data reduction is possible the time it takes to triangulate the transmitter position can be reduced, thus more transmitters can be localized and the efficiency is increased.

1.1 Scope

The nodes in figure 1.1 can have different capability levels, everything from just modulating the signal to another frequency and re-transmitting it to time

[1] A list of abbreviations can be found on page 7.

Media	Transmission rate
Radio link	$\sim$ 1 kbit/s – $\sim$ 50 Mbit/s
Passive laser	$\sim$ 50 Mbit/s
Active laser	$\sim$ 1 Gbit/s
Electrical cable	$\sim$ 1 Gbit/s
Optical cable	$\sim$ 100 Gbit/s

Table 1.1: Transmission rates in different media used in localization systems (Johansson, 2008b, chapter 4).

stamping and processing the data. The latter case is assumed, hence the time needed for compression and transmission to the base node will not introduce a relative delay between the nodes.

This thesis is about compression and localization, not detection and/or demodulation. Therefore, signals will be treated as baseband signals. Implementation and evaluation have been done in MATLAB, even though some actual signal transmissions have been sampled, this thesis has an exploratory focus rather than an implementation focus.

Furthermore, the types of signals investigated have been limited to a few common types, see section 3.3 on page 24 for discussion and signal descriptions. The signals are assumed to be transmitted during the entire sampling time.

Earlier work on the subject includes the works of Mark Fowler among others, but the papers found are either very general (e.g. Fowler (1999), saying compression can be applied to localization systems) or very signal specific (e.g. Fowler *et al.*, which looks at a certain type of radar signals). This thesis aim to investigate rather straight-forward approaches to data compression on common types of signals, and see if they are beneficial.

1.2 Method

To evaluate the different compression schemes utilized in this thesis a simulation model is used. The localization performance using compressed signals is compared against the performance using uncompressed signals. Each simulation is performed 100 times to get a reliable measure of the standard deviation. The simulation test bench is written in MATLAB.

The simulation uses three different signal types, see section 3.3 on page 24. The simulations are also compared against the theoretical limit of the localization performance, see section 2.4 on page 20.

To evaluate how the compression schemes works on recorded data using a real channel, a field experiment was conducted. Two vehicles were used, one equipped with a transmission system and one equipped with a receiving system. The recorded data was used in a modified version of the simulation test bench for evaluation.

1.3 Thesis Disposition

Chapter 1 is this chapter, and aims to briefly explain what this thesis is about, the problem it investigates and why the problem is of interest.

Chapter 2 describes the theory behind TDOA and how it can be used for localization. The localization system used in this thesis is presented and finally a theoretical lower bound for the accuracy of the estimated transmitter position is discussed.

Chapter 3 characterizes the signal types investigated and defines how signal to noise ratio is calculated.

Chapter 4 deals with compression techniques, the transforms and quantization methods used in this thesis. It presents the transform coding model that the thesis rely on. The chapter also depicts decorrelation and compaction. The Cramér-Rao bound is also extended with the distortion from compression.

Chapter 5 shows simulation results and how they where obtained. It presents ratio calculations for the different compression schemes and localization ability adjusted ratio.

Chapter 6 describes a field experiment performed where signals where transmitted and received. It presents how this experiment was conducted, the problems that occurred, and the localization result using the collected data.

Chapter 7 draws conclusions and looks forward.

2 Overview of TDOA

2.1 Introduction

Signal localization can be done in a wide variety of ways Andersson *et al.* (2004a,b), but this thesis will focus exclusively on time difference of arrival (TDOA)[1]. This method relies on the finite propagation speed of the measured signals, resulting in different time of arrival at differently located receivers.

Given two sensors and one transmitted signal, the received signals can be modeled as[2] Knapp & Carter (1976)

$$x_1(t) = s(t) + \nu_1(t) \quad \text{and} \quad x_2(t) = s(t + \Delta) + \nu_2(t), \tag{2.1}$$

with the noise $\nu_1(t)$ and $\nu_2(t)$, uncorrelated to $s(t)$, and the time delay Δ.

From two real-valued signals, the cross correlation function can be calculated as the expected value

$$r_{1\,2}(\tau) = E[x_1(t)x_2(t + \tau)] \tag{2.2}$$

to find the time delay estimator $\hat{\Delta}$ as the τ that maximizes $r_{1\,2}(\tau)$. Given the geometry for the sensor pair together with the estimated $\hat{\Delta}$, the position of the transmitter is known to be somewhere along a hyperbola Andersson *et al.* (2004b) with equation

$$|\mathbf{p}_1 - \mathbf{q}| - |\mathbf{p}_2 - \mathbf{q}| = \hat{\Delta}c, \tag{2.3}$$

where $\mathbf{p}_1$ and $\mathbf{p}_2$ are the receiver positions, $\mathbf{q}$ is the sought transmitter position and c is the propagation speed. This is illustrated in figure 2.1, where each

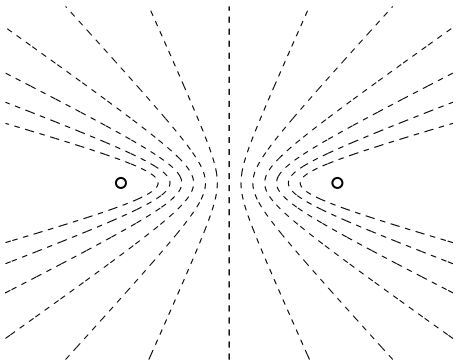

Figure 2.1: Two receivers, each hyperbola corresponds to an estimated time delay $\hat{\Delta}$.

hyperbola corresponds to an estimated $\hat{\Delta}$.

2.2 Localization Using TDOA

In general, localization is a difficult problem. Therefore, some simpler models are needed, which provide useful tools to investigate localization properties.

[1] Sometimes referred to as *time delay of arrival*.

[2] Without regard to attenuation.

In free space propagation without attenuation, which is the only propagation model used in this thesis, the channel can be modeled as a function of time delay. Attenuation can be thought of as a lowered signal to noise ratio (SNR) level, and is therefore not necessary for the setup described in section 2.3. Between a signal transmitter q and a receiver p, the channel impulse response becomes (Johansson, 2008a, part 4)

$$h_{q\,p}(t) = \delta\left(t - \frac{\|\mathbf{p}-\mathbf{q}\|}{c}\right) = \delta\left(t-\Delta\right) \tag{2.4}$$

in the time domain and the channel system function

$$H_{q\,p}(\omega) = \exp\left(\frac{-j\omega\|\mathbf{p}-\mathbf{q}\|}{c}\right) = \exp\left(-j\omega\Delta\right) \tag{2.5}$$

in the Fourier domain. Here, $\mathbf{p}$ and $\mathbf{q}$ are the position vectors of p and q, respectively, $\delta(t)$ is the Dirac's delta function, and c is the propagation speed. In this case, c is the speed of light. The measured signal at p can then be modeled as

$$x(t) = s(t) * h_{q\,p}(t) + \nu_p(t), \tag{2.6}$$

where $s(t)$ is the transmitted signal and $\nu_p(t)$ is the noise[3].

Given two received signals x_m and x_n from a sensor pair p_m and p_n, the cross spectral density function between the signals can be formulated as

$$S_{m\,n}(\omega) = \mathcal{F}\left\{r_{m\,n}(\tau)\right\} = \mathcal{F}\left\{E[x_m(t)x_n(t+\tau)]\right\}, \tag{2.7}$$

where $r_{m\,n}(\tau)$ is the cross-correlation function between x_m and x_n. The reasons to take the Fourier transform are practical. One might wish to do Fourier domain signal processing before sending the signal to the localization system, and the computation complexity of a cross-spectral density is significantly less than that of a convolution.

Using (2.6) and (2.7) together with the cross spectral density output of a linear system[4] it can be rewritten as

$$S_{m\,n}(\omega) = \mathcal{F}\left\{E[s(t)s(t+\tau)] * h_m(t) * h_n(-t) + E[\nu_m(t)\nu_n(t+\tau)]\right\}. \tag{2.8}$$

The Fourier transform is then applied and the result is

$$S_{m\,n}(\omega) = S_s(\omega)H_m(\omega)H_n^*(\omega) + S_{\nu_m\,\nu_n}(\omega). \tag{2.9}$$

Then, using (2.5),

$$\begin{aligned} S_{m\,n}(\omega) &= S_s(\omega)e^{-j\omega\Delta_m}e^{j\omega\Delta_n} + S_{\nu_m\,\nu_n}(\omega) \\ &= S_s(\omega)e^{-j\omega(\Delta_m-\Delta_n)} + S_{\nu_m\,\nu_n}(\omega) \\ &= S_s(\omega)e^{j\omega\Delta_{m,n}(\mathbf{q})} + S_{\nu_m\,\nu_n}(\omega) \end{aligned} \tag{2.10}$$

where $\Delta_{m,n}(\mathbf{q})$ is the TDOA, for the signal $s(t)$ from transmitter q, between p_m and p_n.

It is not sufficient using only two receivers to locate a signal source on a two dimensional plane using TDOA. Figure 2.2 on the facing page shows a linear array setup with three receivers. Linear arrays setups are seldom used in reality, in part because there is a false mirror interception point, and the accuracy along an imagined y-axis is rather poor.

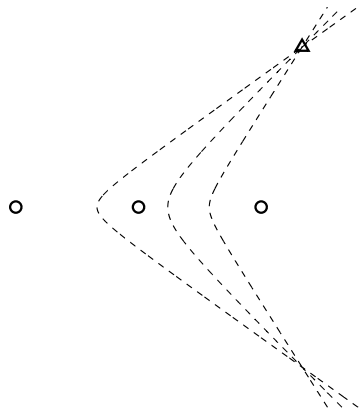

Figure 2.2: Three receivers locating one transmitter using TDOA.

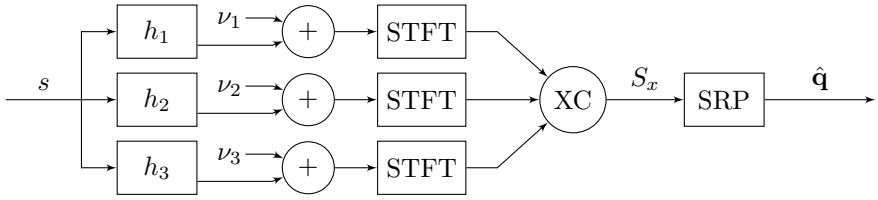

Figure 2.3: Localization system using TDOA and cross correlation (XC).

2.3 Experiment Model

MATLAB is used to establish a test bench for verification. The setup, a rather simple symmetrical case, is shown in figure 2.4 on the next page, with receivers p_1, p_2 and p_3 and the transmitter q. All receivers are equidistant from the transmitter and distributed evenly around the transmitter, forming a circle. The reason for such a symmetric setup is to introduce symmetry of the error distribution, simplifying the Cramér-Rao bound (CRB) (see section 2.4 on page 20). TDOA localization works well in an asymmetrical setup as well, as long as the problem illustrated in figure 2.2, that the localization ability becomes one-dimensional, do not arise. This experimental model will not consider multi-path propagation.

The distance from the transmitter to the receivers is $\sqrt{3} \cdot 10$ km. This distance is arbitrary, but a sensor array small enough to avoid multiple solutions is desirable, a localization scheme looking at the phase data will have a hard time differentiating between solutions separated by a whole wavelength. A signal bandwidth much smaller than the propagation speed c divided by the largest distance in the receiver array, is desirable Cook (2003). The minimum distance is limited by the time synchronization and self localization ability of the system.

The transmitted signal s is filtered with the channels impulse response described in (2.4) on the facing page. When the signal has passed the channel, uncorrelated noise is added independently to each signal, amplitude scaled to get the desired SNR (see section 3.1 on page 23).

[3] $*$ denotes convolution, see symbol list on page 9.
[4] See e.g. (Pursley, 2002, page 68).

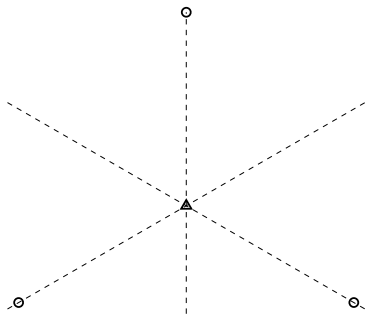

Figure 2.4: Experiment setup displaying the three receivers as circles and the transmitter as a triangle. The distance between the transmitter and receivers are $\sqrt{3} \cdot 10$ km and the receivers are evenly distributed around the transmitter forming a circle.

To estimate the cross-spectral density the signal is first transformed using short-time Fourier transform (STFT) described below

$$\mathrm{STFT}\left\{x(n)\right\} = X(l,\omega) = \sum_{n=-\infty}^{\infty} x(n - L_B l) w(n) e^{-j\omega n}. \tag{2.11}$$

The STFT divides the signal into L blocks of length L_B with the Hamming window w,

$$w(n) = 0.54 - 0.46 \cos\left(\frac{2\pi n}{L_B - 1}\right), \tag{2.12}$$

and performs the discrete Fourier transform of every block. Each block overlaps the preceding one with 50%, this is ideal when using the Hamming window since the sum of all windowed blocks will produce the original signal.

The cross-spectral density between the signals is then estimated for every sensor pair according to

$$S_{m,n}(\omega_k) = \frac{1}{L} \sum_{l=1}^{L} X_m(l,\omega_k) X_n^*(l,\omega_k). \tag{2.13}$$

where the indexes m and n denotes the received signal at p_n and p_m, respectively. X^* denotes the conjugate transpose[5] of X. ω_k is the angular frequency with index k.

The last step is to locate the position of the transmitter from the estimated cross-spectral density. This is done by using the steered response power (SRP). Different approaches can be taken here, see e.g. (Johansson, 2008a, part 4) for alternate methods. Steered response power (SRP) is a well used and robust method for localization Dmochowski *et al.* (2007) and suitable to be used in this experiment. Given the estimated cross-spectral density the SRP at the position $\mathbf{u}$ is in this case

$$P(\omega_k, \mathbf{u}) = \sum_{m=1}^{M} \sum_{n=1}^{M} S_{m,n}(\omega_k) e^{-j\omega_k \Delta_{m,n}(\mathbf{u})}. \tag{2.14}$$

[5]Sometimes called the *Hermitian transpose*.

$\Delta_{m,n}(\mathbf{u})$ is the TDOA for transmitting a signal from position $\mathbf{u}$ to receivers p_m and p_n. By using (2.10) on page 16 and an ideal noise free scenario the SRP is

$$\begin{aligned} P(\omega_k, \mathbf{u}) &= \sum_{m=1}^{3}\sum_{n=1}^{3} S_s e^{j\omega_k \Delta_{m,n}(\mathbf{q})} e^{-j\omega_k \Delta_{m,n}(\mathbf{u})} \\ &= \sum_{m=1}^{3}\sum_{n=1}^{3} S_s e^{j\omega_k (\Delta_{m,n}(\mathbf{q}) - \Delta_{m,n}(\mathbf{u}))}. \end{aligned} \tag{2.15}$$

It can be shown that in an ideal noise free scenario $\max_{\mathbf{u}} P(\omega_k, \mathbf{u})$ can be found at, and only at, $\mathbf{u} = \mathbf{q}$ Johansson (2008a). Figure 2.5 shows the amplitude scaled magnitude of the frequency average SRP in the experiment scenario, i.e.

$$\left| \sum_k P(\omega_k, \mathbf{u}) \right|. \tag{2.16}$$

The peak is found at the position of the transmitter, where

$$\mathbf{u} = \mathbf{q} \implies e^{j\omega_k (\Delta_{m,n}(\mathbf{q}) - \Delta_{m,n}(\mathbf{u}))} = 1. \tag{2.17}$$

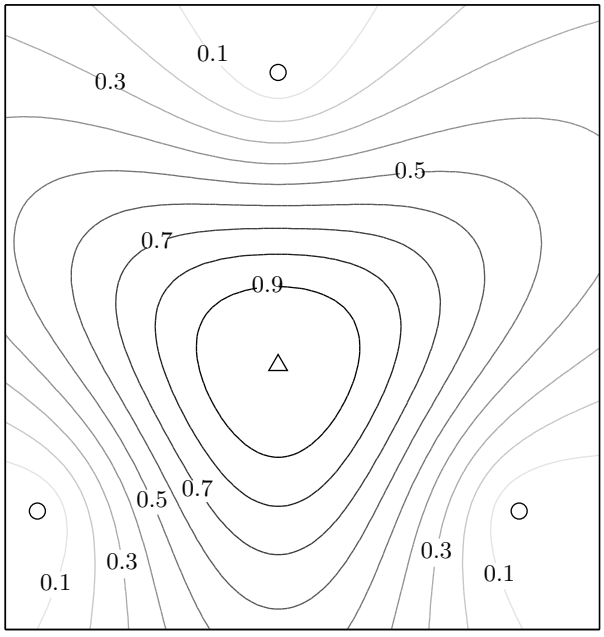

Figure 2.5: The magnitude of a SRP scaled between 0.0 and 1.0 illustrated with contour lines. The receivers are illustrated as circles and the transmitter as a triangle.

In section 2.4 on the following page, it will be shown that there is a fundamental limit to how good an estimator can be, called the Cramér-Rao bound (CRB). This bound is used in this thesis to determine the number of time samples needed for a reasonable precision of flat spectrum signal localization (see section 3.3.1 on page 24).

2.4 The Cramér-Rao Bound

There exists a theoretical lower bound for the variance of the error in the estimated location of a transmitter Knapp & Carter (1976). When estimating the position from a finite recorded data set the variance of the estimation error is dependent on a matrix $\mathbf{J}$, which is called the Fisher information matrix (FIM)[6] Johansson (2008b). This matrix can be used to set a theoretical lower bound for the accuracy of a localization system. The inverse of FIM is called the Cramér-Rao matrix bound (CRMB) and can be used to geometrically describe the variance of the localization error in a system. The FIM, with respect to TDOA, for a flat spectrum baseband signal is (Johansson, 2008b, chapter 11)

$$\mathbf{J} = \frac{T}{2\pi} \cdot \frac{B^3}{6} \cdot \frac{(\text{SNR})^2}{1 + M \cdot (\text{SNR})} \cdot \frac{1}{c^2} \cdot \mathbf{G}\mathbf{G}^T, \tag{2.18}$$

where B is the bandwidth of the signal, SNR is the signal-to-noise gain ratio, and $\mathbf{G}\mathbf{G}^T$ is a matrix dependent on the sensor array. If N is the number of signal samples, the measured time becomes

$$T = \frac{N2\pi}{B}$$

so $\mathbf{J}$ can be also be expressed as

$$\mathbf{J} = \frac{NB^2}{6} \cdot \frac{(\text{SNR})^2}{1 + M \cdot (\text{SNR})} \cdot \frac{1}{c^2} \cdot \mathbf{G}\mathbf{G}^T, \tag{2.19}$$

For the propagation model used in this thesis $\mathbf{G}\mathbf{G}^T$ is

$$\mathbf{G}\mathbf{G}^T = \mathbf{g}(M\mathbf{I} - \mathbf{1})\mathbf{g}^T, \tag{2.20}$$

where $\mathbf{I}$ is the identity matrix, $\mathbf{1}$ is a matrix of ones and the matrix $\mathbf{g}$ is a function of the positions of the transmitter q and receivers p_m. In the simulation scenario with 3 receivers p_m and one transmitter q the matrix $\mathbf{g}$, with the direction to each transmitter along its rows, is

$$\mathbf{g} = \begin{bmatrix} \frac{\mathbf{q}-\mathbf{p_1}}{||\mathbf{q}-\mathbf{p_1}||} & \frac{\mathbf{q}-\mathbf{p_2}}{||\mathbf{q}-\mathbf{p_2}||} & \frac{\mathbf{q}-\mathbf{p_3}}{||\mathbf{q}-\mathbf{p_3}||} \end{bmatrix}. \tag{2.21}$$

Note that this matrix does not contain any information about the distances, only the direction to receivers from the transmitter.

The Cramér-Rao matrix bound (CRMB) follows as

$$\text{CRMB} = \mathbf{J}^{-1}. \tag{2.22}$$

As mentioned, the CRMB geometrically describes the variance in the localization error. In the symmetric simulation scenario described in section 5.1 on page 45, this matrix will not only be diagonal, but have the same value in all positions along the diagonal. Hence, it is useful to speak of *the* Cramér-Rao bound (CRB), referring to one of these identical elements. The standard deviation, the square root of the variance, can be expressed in meters, and is therefore the most useful measurement to relate evaluation results to.

The CRB is only a theoretical bound that rarely is reached in real life scenarios, however it tells a lot about the trend of the localization error. One can note that the error variance will be proportional to the reciprocal of T, B^3, and have a proportional trend for SNR (in gain). In this thesis the CRB is used together with the calculated standard deviations from simulation to compare the trends. Figure 2.6 on the next page shows the lower standard deviation bound for a 1 kHz signal using different measured times, T.

[6] The Fisher information matrix (FIM) is a general measure of variance of the score of the given estimator. For more details, see (Cover & Thomas, 2006, chapter 11).

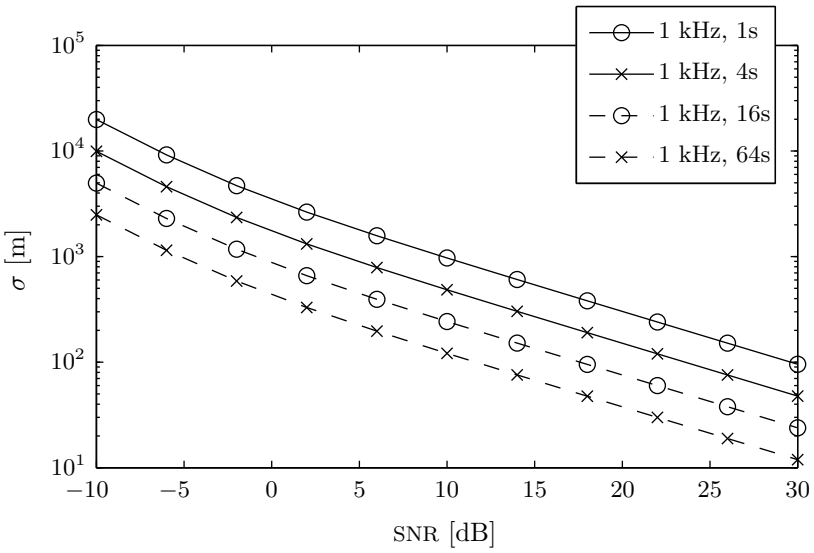

Figure 2.6: CRB for FSS, 1 kHz signal bandwidth at different signal lengths using SNR levels from −10 to 30 dB.

3 Signals

The signals used for compression in this thesis are baseband signals, i.e. have been demodulated before entering the system. This assumes that there is some kind of intelligence prior to the localization, e.g. an operator or an automatic system that can identify the presence of a signal. The aim of this thesis is localization, not detection. The channel is assumed to be a Gaussian channel (Cover & Thomas, 2006, chapter 9), as depicted in figure 3.1

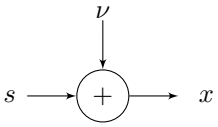

Figure 3.1: Gaussian channel.

3.1 Signal to Noise Ratio

Signals with different signal to noise ratio (SNR) is generated by adding white Gaussian noise (WGN) to the original signal. WGN is generated and the power is estimated as

$$P_x = \frac{1}{N}\sum_{n}^{N} |x(n)|^2 \tag{3.1}$$

for both the original signal s and and the noise ν. The noise is then multiplied with an appropriate coefficient κ and added to the signal to get the desired SNR. The SNR is defined as

$$\text{SNR} = 10\log_{10}\left(\frac{P_s}{P_\nu}\right) \tag{3.2}$$

and the coefficient, κ, is calculated using

$$\kappa = \sqrt{\frac{P_s}{P_\nu}\cdot 10^{-\text{SNR}/10}}. \tag{3.3}$$

The SNR range used is between -10 dB and 30 dB, this approximate range is commonly used when illustrating the performance of TDOA[1].

3.2 Signal and Noise Spectrum

Throughout this thesis, the noise will have more or less the same energy distribution, WGN, but the signals will not always have a distribution that resembles the noise. This is important to take into consideration when interpreting signal bandwidth and SNR. When considering a single node receiving a single side band (SSB) signal with 0 dB SNR, the signal might be easy to distinguish from the noise, while a flat spectrum signal (FSS) will not.

[1] See e.g. Falk (2004), Fowler *et al.* (2005), or Johansson (2008a).

SNR	2 kHz	10 kHz	20 kHz	30 kHz	300 kHz
-10 dB	$9.9 \cdot 10^6$	$3.9 \cdot 10^5$	$9.9 \cdot 10^4$	$4.4 \cdot 10^4$	440
0 dB	$3.0 \cdot 10^5$	$1.2 \cdot 10^4$	$3.0 \cdot 10^3$	$1.3 \cdot 10^3$	13
10 dB	$2.4 \cdot 10^4$	940	240	100	10
20 dB	$2.3 \cdot 10^3$	91	23	10	< 10
30 dB	230	< 10	< 10	< 10	< 10

Table 3.1: The number of samples needed for flat spectrum signals at different bandwidths and SNR levels for 100 meter standard deviation CRB. Note that data compression on wide bandwidth signals with high SNR is not necessary due to the small amount of data needed.

3.3 Signals of Interest

There is a practically unlimited numbers of signals that can be sent, so there is a need to limit the range of signals to study. First, there is the limit mentioned above, that only baseband signals are considered. Secondly, the study is limited to the following signal types, more on that in the appropriate sections.

- Flat spectrum signals (FSSs), see section 3.3.1. This is a very general signal model.
- Phase-shift keying (PSK) signals, see section 3.3.2 on page 26. Commonly used by data modems.
- Single side band (SSB) signals, see section 3.3.3 on page 27. Used by some walkie-talkie systems.

Furthermore, narrow bandwidth signals are more interesting because they require more data to be used when estimating TDOA (this follows from the CRB, see section 2.4 on page 20). Table 3.1 shows the number of samples needed for signals at different bandwidth and different SNR. It can be seen that for higher bandwidth signals the number of samples needed is small, therefore no compression is needed.

3.3.1 Flat Spectrum Signals

A signal resembling white Gaussian noise (WGN) is the most general signal model there is. Many communication channels can be modeled as Gaussian channels, and it can be shown that the most efficient use (achieving channel capacity) of such a channel is to send signals with a Gaussian distribution (Cover & Thomas, 2006, chapter 9).

The FSSs used in this thesis are complex-valued and bandwidth limited, generated by MATLAB's pseudo-random `randn` by generating the real valued and complex valued parts separately.

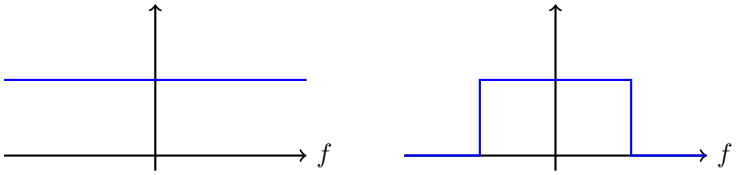

(a) White Gaussian noise

(b) Bandwidth limited flat spectrum signal

Figure 3.2: Frequency energy distributions for WGN and bandwidth limited FSS.

3.3.2 Phase-Shift Keying

A modulated bandpass signal can be modeled as Carlson (2002)

$$x(t) = A_c[x_i(t)\cos(\omega_c t + \theta) - x_q(t)\sin(\omega_c t + \theta)] \tag{3.4}$$

with the coded message contained in the in-phase component $x_i(t)$ and the quadrature component $x_q(t)$.

Phase-shift keying (PSK) is a way to modulate digital signals by placing a number of code words around the unit circle in the in-phase/quadrature plane. 8-PSK and 4-PSK are common signal types used in simple data modems, where 4 and 8 is the number of code words used. Figure 3.3 shows the signal constellation for such signals.

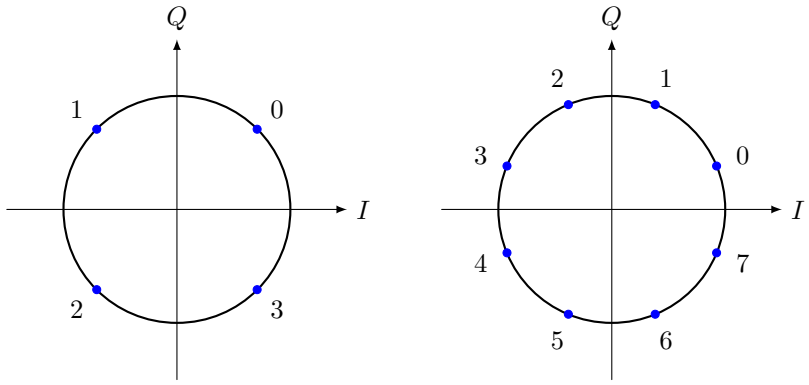

(a) 4-PSK (Q-PSK) (b) 8-PSK

Figure 3.3: Examples of phase-shift keying signal constellations in the in-phase/quadrature plane.

3.3.3 Amplitude Modulated Signal Side Band

An AM-SSB is constructed from an amplitude modulation (AM) signal, suppressing its carrier wave and one of the sidebands. This is an energy and bandwidth efficient use of AM, but is harder to properly synchronize on the receiver side (Carlson, 2002, chapter 4.5). This type of signal is commonly used by radio amateurs and for long distance voice radio transmission in some systems.

A simple baseband representation of a single side band (SSB)-like signal with bandwidth B can be constructed by "demodulating" an ordinary wave audio file by $B/2$, run through a low-pass filter with $\pm B/2$ cut-off frequencies and resample it. This is illustrated in figure 3.4. Note that the resulting signal is complex valued. The SSB signals used in this thesis are created in this manner from an audio book source.

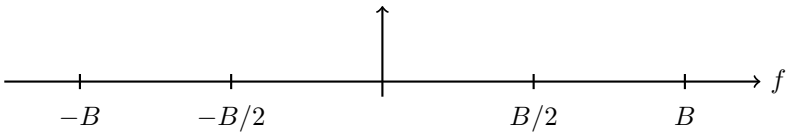

(a) Audio file (mixed sound channels)

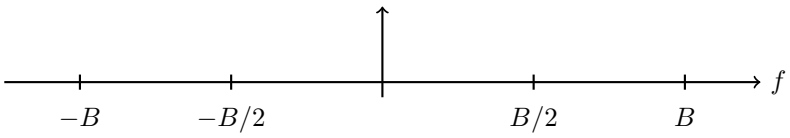

(b) Demodulated signal

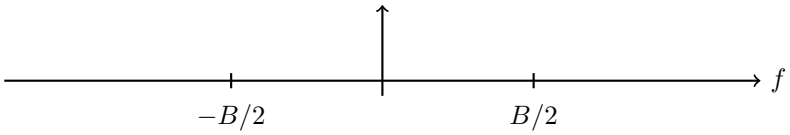

(c) Low-pass filtered SSB ready for use

Figure 3.4: Schematic frequency distributions of stages in single side band signal creation.

4 Compression of signal data

To estimate the location of a transmitter each sampled signal needs to be transferred to a shared resource where the signals can be correlated. The capacity of the channel between the receivers is limited Johansson (2008b), see table 1.1 on page 12.

A compression algorithm is sought that keep data relevant for TDOA and discard irrelevant data. If such an algorithm is found it is possible to reduce the amount of data needed to be sent from the receiving nodes and this gives the possibility to estimate the position of more transmitters for the given communication resources.

4.1 Transform Coding

Transform coding is a technique in which the data is transformed into components. These components can then be sent over the given channel; the receiver can then transform the components back to its original base and thus recreate the signal.

Since Hotelling's paper in 1933 Hotelling (1933), the first to describe principal component analysis, different transforms have been used to better capture the characteristics of a given signal.

By choosing the used transform base carefully it is possible to achieve results where most of the signal information is compacted into only a few components. These components are then sent over the link, but the components with little or no information are discarded. A good estimate of the signal can then be recreated at the receiver. Transform coding can also achieve decorrelation, so that the redundancy between data points is reduced. Reducing redundancy might be a problem if the communication from the nodes to the base system suffers data loss. This is probably better handled by the use of error correcting codes rather than skipping compression, but is outside the scope of this thesis.

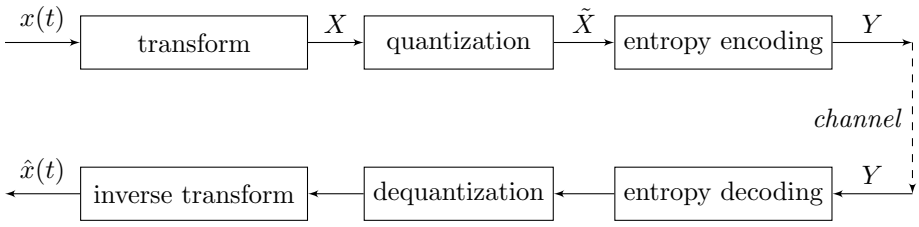

Figure 4.1: Transform coding compression.

Figure 4.1 describes a system using transform coding for data compression. The signal $x(t)$ is transformed and then quantized in a way that preserves the characteristics of the signal most interesting to the application, e.g. signal variance, signal energy, or some other measure of perceived quality. The quantized signal is then entropy coded, with e.g. Huffman coding, and sent over the channel. The signal is then decoded, dequantized and re-transformed to its original base to get the estimate $\hat{x}(t)$.

4.1.1 Illustration of Decorrelation

The auto-correlation matrix of a sampled signal x is defined as

$$R_x = E[xx^*]. \tag{4.1}$$

A nice way to illustrate transform decorrelation efficiency is by looking at the auto-correlation matrix R_x for the signal at hand.

Algorithm 4.1: Transformation of R_x

1. Generate signal x
2. Rearrange x into blocks of length L_B, placing them as rows of χ
3. Calculate the auto-correlation matrix $R_\chi = E[\chi\chi^*]$
4. If desired, change basis using the transform T, $R_y = TR_\chi T^{-1}$
5. Normalize and plot R_y

Figures 4.2 to 4.5 on pages 32–33 serves as examples of such an illustration, using a SSB speech signal. Decorrelation shows up as diagonally dominant matrices, complete decorrelation is a diagonal R_y. The Karhunen-Loéve transform (KLT) achieves this Algazi & Sakrison (1969), see figure 4.3 on page 32. In this figure we also have high energy compaction to few components, indicating a compression-friendly signal.

4.1.2 Karhunen-Loéve Transform

Principal component analysis (PCA) of a signal is performed by looking at the eigenvalue decomposition of the auto-correlation matrix. This captures many characteristics of the given signal and effectively ranking them, the transform puts the most energy in the fewest components (Rao & Yip, 1990, chapter 3). Then, we can reduce the amount of data by only transmitting the eigenvectors belonging to the largest eigenvalues, and one symbol for each such component per signal block.

The Karhunen-Loéve transform (KLT), with the eigenvectors of the auto-correlation matrix along its columns, is an example of a PCA transform.

This transform provides the largest transform coding gain of any transform method. It minimizes the mean squared error for the given number of components, but has a large overhead (Sayood, 2005, chapter 13.4), since each used eigenvector has to be transmitted. This overhead can remove the advantages of this optimal transform and make it impractical to use for compression. It is still interesting from a theoretical point of view but other transform methods may be needed that do not depend on the data being sent.

4.1.3 Discrete Cosine Transform

The discrete cosine transform (DCT) type 2[1] transforms $x(k)$ to $X(m)$ as

$$X(m) = \sum_{k=0}^{N-1} x(k) \cos\left[\frac{\pi}{N} m \left(k + \frac{1}{2}\right)\right] \tag{4.2}$$

[1] Only the DCT type 2 is considered. For different types of DCT, see Rao & Yip (1990).

where N is the block length[2], with an inverse transform

$$x(k) = \frac{X(0)}{2} + \sum_{m=1}^{n-1} X(m) \cos\left[\frac{\pi}{N} m \left(k + \frac{1}{2}\right)\right]. \tag{4.3}$$

The big advantage of the DCT compared to the KLT (see section 4.1.2) is that the transform matrix is not signal dependent, and therefore does not need to be transmitted. Asymptotically, if the signal is Markovian, the DCT is equivalent to KLT as the correlation coefficient $\rho \to 1$ (or $\rho \to 0$, since the auto-correlation matrix is then diagonal). Similarly, as the matrix size $N \to \infty$ (and thus the block length), the DCT is equivalent to the KLT. (Rao & Yip, 1990, chapter 3.3–4)

4.1.4 Discrete Fourier Transform

The DCT, described in 4.1.3 on the preceding page, is a special case of the discrete Fourier transform (DFT) for real-valued functions. The DFT is defined as

$$X(k) = \sum_{n=0}^{N-1} x(n) \exp\left(\frac{-2\pi jnk}{N}\right) \tag{4.4}$$

and its inverse as

$$x(n) = \frac{1}{N} \sum_{k=0}^{N-1} X(k) \exp\left(\frac{2\pi jnk}{N}\right). \tag{4.5}$$

The short-time Fourier transform (STFT) is a time limited DFT, essentially performing the transform at the signal one block at a time, see section 2.3. This scheme is used in the localization system so some synergy can be found here. Instead of applying the inverse transform before localization, we can skip this step. Although of little importance for localization properties in theory, it helps to rid simulations of block effects (see section 5.1.3 on page 47) and will save computation time.

[2]Note that N indicates the number of samples transformed rather than the block length, but since a transform is often applied to one block at a time, the number of samples N is the same as the block length, from the transform's point of view.

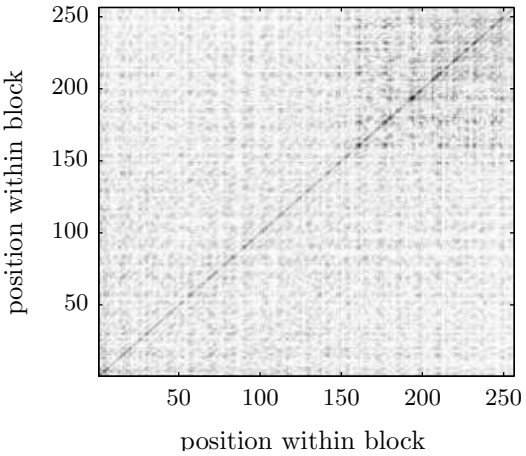

Figure 4.2: Illustration of the magnitude of the auto-correlation matrix R_χ of a SSB signal. See algorithm 4.1 on page 30. Darker color illustrates higher magnitude.

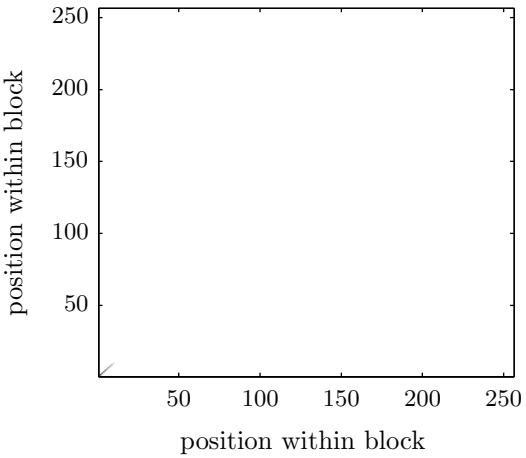

Figure 4.3: Illustration of the magnitude of the transformed auto-correlation matrix R_χ using Karhunen-Loéve transform of a SSB signal. Darker color illustrates higher magnitude. The components are arranged by eigenvalue magnitude, all energy is compacted in the lower left corner. Since there is no energy outside the diagonal, complete decorrelation is achieved.

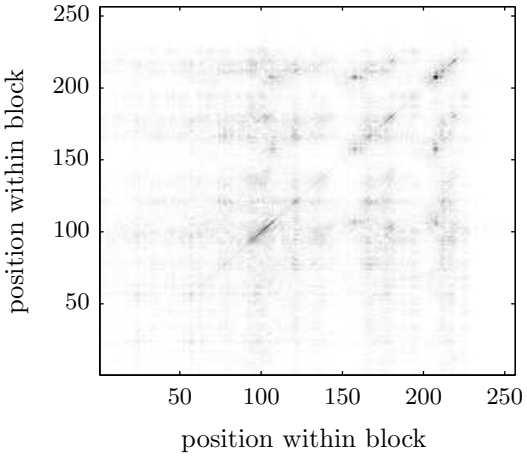

Figure 4.4: Illustration of the magnitude of the transformed auto-correlation matrix R_χ using Discrete cosine transform of a SSB signal. Darker color illustrates higher magnitude. The components are arranged by frequency, from low to high.

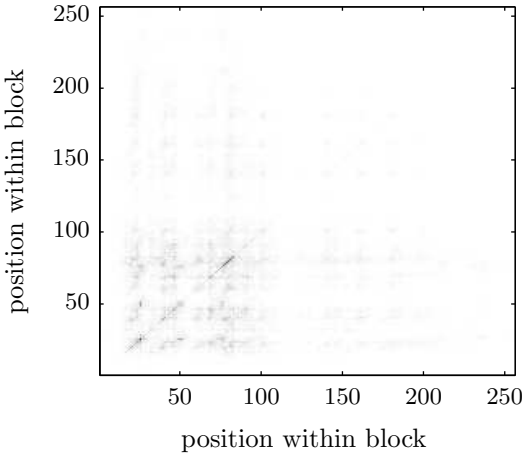

Figure 4.5: Illustration of the magnitude of the transformed auto-correlation matrix R_χ using Discrete Fourier transform of a SSB signal. Darker color illustrates higher magnitude. The components are arranged by frequency, from negative to positive.

4.2 Quantization

When an appropriate transform method has been established the data needs to be quantized, i.e. truncated to a number of data levels, see figure 4.1 on page 29. First, 8 bit values are used (see section 5.1.2 on page 46). Then some method for selecting which data to keep is applied. Both these steps are referred to as *quantization*, and is where most of the actual compression occurs. The transform step will only point out which data to cut in the quantization step.

In this thesis three different approaches are used for quantization; integral components (section 4.2.1), keeping partial components (section 4.2.2) and time-frequency masking (section 4.2.3). This section aims to describe these approaches. For example compression ratio calculations, see section 5.1.5 on page 48.

4.2.1 Integral components

First off is the integral components method. The approach for this quantization is to throw away transform components insignificant to TDOA localization. Components with high energy, containing phase information relevant for estimating the TDOA, are transmitted uncompressed. Which components to select turns out to be non-trivial in a noisy environment, as illustrated in section 4.2.1.1.

The quantization is done by sorting the transform components by the average energy over all transform blocks and discard components based on the desired compression ratio.

Since the method decides which components to keep based on the average signal energy in all blocks it is possible that insignificant samples are kept e.g. during silent time periods in a speech signal.

4.2.1.1 The Component Selection Problem

If all three receivers select transform components by signal energy, independently from each other, they might not select the same components in a noisy environment. This can be mitigated by a protocol allowing the nodes to agree on a set of transform components to use. Such a protocol is assumed not to be allowed here. Figure 4.6 on the next page is the result of a simulation with 1000 iterations as described in algorithm 4.2. The noiseless curve (∞ dB SNR) is not simulated, but added for clarity.

Algorithm 4.2: DFT component selection on FSS

1. Generate a flat spectrum signal (see 3.3.1 on page 24).
2. Create three received signals by adding uncorrelated noise to get the desired SNR.
3. Run signal through DFT with block length 128.
4. Choose K components of each transformed signal, according to signal energy.
5. Find the number of components chosen for all three signals.

As seen in figure 4.7 on the facing page, selecting components by signal energy

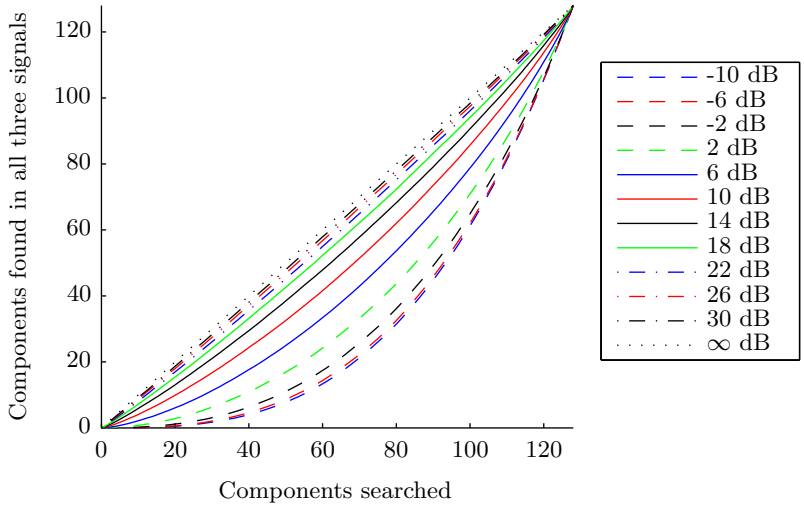

Figure 4.6: Average number of components chosen in three flat spectrum signal per dB SNR.

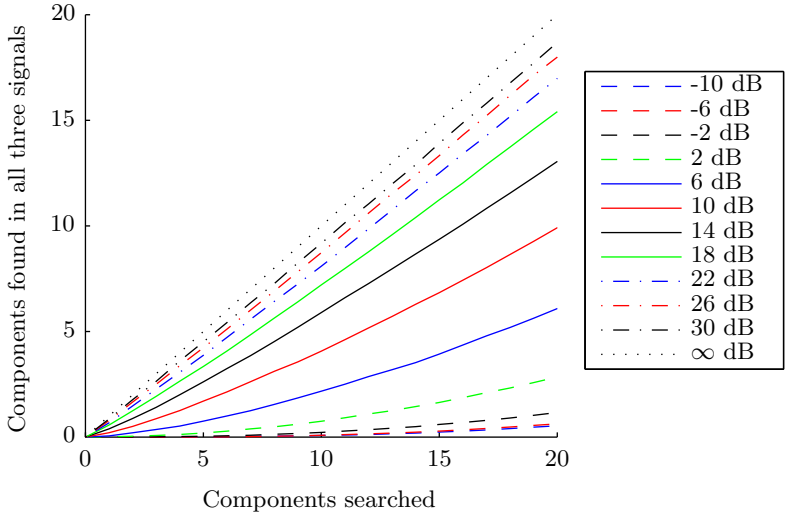

Figure 4.7: Average number of components chosen in three flat spectrum signal per dB SNR. Zoomed in at few selected components.

independently is not a good approach for WGN-like signals. With a reasonable amount of components to acquire an adequate compression rate, say 10, we have very few common components[3] for a SNR below 10 dB. Thus, this method seems useless for flat spectrum signals in white Gaussian noise, which was also confirmed by simulations (see section 5.2.1 on page 50).

For other types of signals, that has a distribution that differs more from the background noise, similar methods provide much better results. Figure 4.8 on the facing page is the result of a simulation with 1000 iterations as described in algorithm 4.3, similar to algorithm 4.2 on page 34 with the notable difference in the first step.

Algorithm 4.3: DFT component selection on SSB signal

1. Generate a SSB speech signal (see section 3.3.3 on page 27).
2. *Continued as algorithm 4.2 on page 34.*

As can be seen clearly in figure 4.9 on the next page, selecting components by signal energy can be done independently in each node with a high degree of certainty that we will choose the same components in all three nodes, for a reasonable number of components.

This implies that for signals that differs in distribution from the noise, this is less of a problem. Similar uncertainty can be found for other quantization schemes, but is most obvious when keeping or discarding integral components.

[3] An interesting note is that the standard deviation is quite small, never above 5 components for the simulation described.

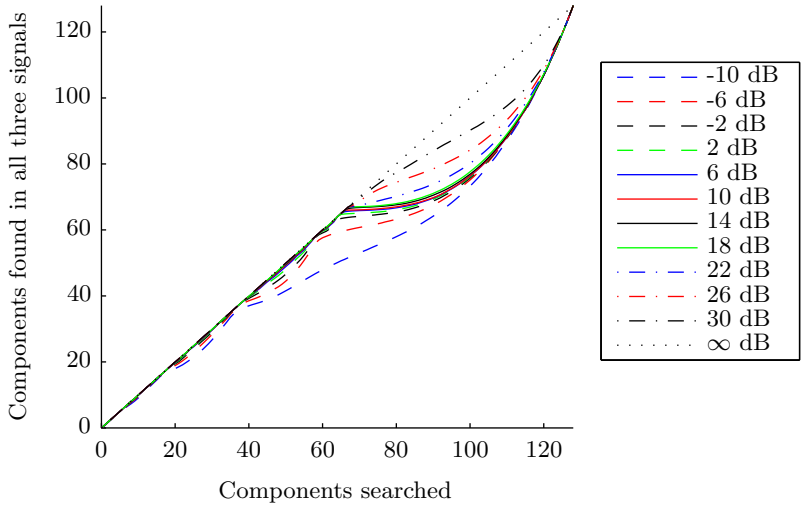

Figure 4.8: Average number of components chosen in three SSB signals per dB SNR.

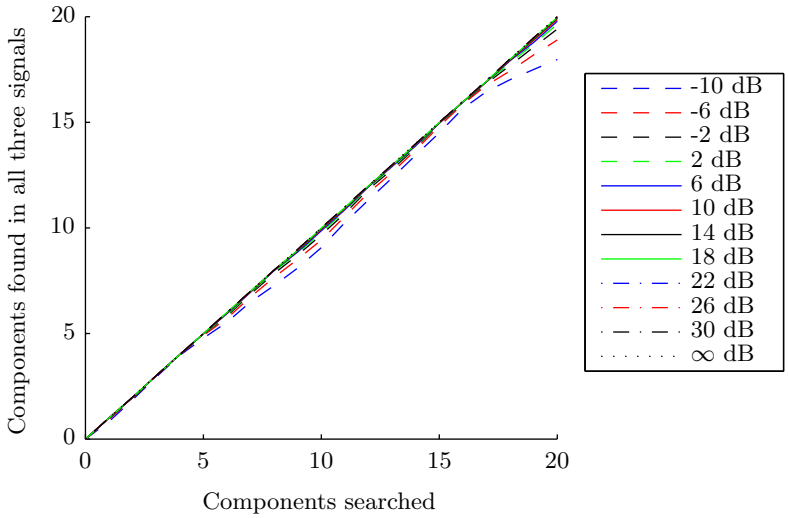

Figure 4.9: Average number of components chosen in three SSB signals per dB SNR. Zoomed in at few selected components.

4.2.2 Partial Components

It is possible to assign different number of bits to different components in the transform domain when performing quantization. One approach is to give the components with higher variance more bits than components with little or no variance. Assuming that components with higher variance contains more relevant information than components with less variance, this method keeps desired properties of the signal.

Equation (4.6) optimally assigns bits and minimizes the reconstruction error of the signal (Sayood, 2005, chapter 13.5).

$$R_k = R + \frac{1}{2}\log_2 \frac{\sigma_k^2}{\prod_{i=1}^{L_b}(\sigma_i^2)^{1/L_B}} \tag{4.6}$$

where σ_k^2 is the variance for component k. R_k is the bits assigned to each component k, R is the average number of bits available for assignment and L_B is the total number of components. However, R_k are not guaranteed to be neither integers or positive. Another approach is to use a recursive algorithm 4.4. In this thesis all signals are assumed to be zero mean signals, hence power and variance are interchangeable. The algorithm therefore assign bits based on power instead of variance.

Algorithm 4.4: Zonal sampling, signal power

1. Compute P_k for each component.
2. Set $R_k = 0$ for all k and set $R_b = L_B R$ where R_b is the total number of bits available for distribution.
3. Sort the energy P_k. Suppose P_1 is maximum.
4. If R_1 is less than 8 increment it by 1, and divide P_1 by 2. If not, proceed with the next highest energy component until a k such that $R_k < 8$ is found.
5. Decrement R_b by 1. If $R_b = 0$ then stop; otherwise go to 3.

This bit allocation scheme is called zonal sampling (Sayood, 2005, chapter 13.5). One drawback of this method is that it assigns bits based on average values, therefore it is possible that samples with insignificant information will be assigned bits. E.g. a speech signal will be assigned bits to transform components with high average variance even within a time period of silence.

When bits have been assigned quantization is performed. If R_k bits are assigned the number of levels the bits can represent becomes 2^{R_k}. The phase is quantized using uniformed quantization, an example of the output of the phase quantization can be found in figure 4.10 on the facing page. The figure shows quantization with 4 bits, the number of output levels then becomes $2^4 = 16$.

The amplitude data is handled in another way. It is scaled between 0 and $2^{R_{\text{MAX}}} - 1$, where R_{MAX} is the largest number of bits assigned to a component. Each sample is then rounded to an integer and then set to the minimum of the rounded value and $2^{R_k} - 1$, where R_k is the bits assigned to the samples corresponding transform component. This assures that any symbol corresponding to a component can be described by the assigned bits. The output of the quantifier can be found in figure 4.11 on page 40. If the amplitude data were to be subjected to the same quantization scheme as the phase data, components with

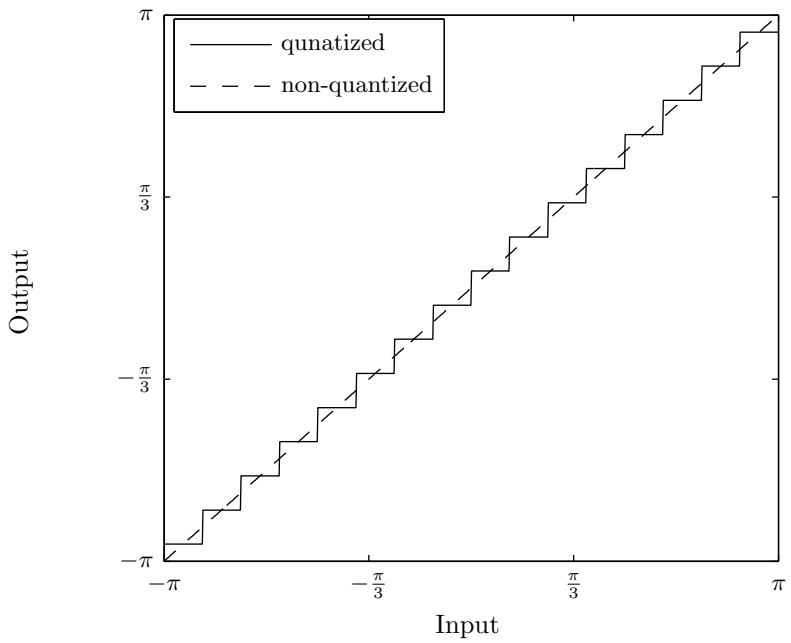

Figure 4.10: Phase input and output of a quantifier using 4 bits. The output is fitted to $2^4 = 16$ levels between $-\pi$ and π.

low average energy might be weighted unfairly high in some blocks, distorting the cross correlation.

4.2.3 Compression Using Time-Frequency Masking

For some non-noise like signals the energy is not distributed evenly in time and frequency, islands of energy appear. This can be seen in figure 4.12 on page 41, which shows the energy distribution in the STFT of a SSB speech signal. In other signals, e.g. a 4-PSK signal, the energy is evenly distributed in the frequency domain over time. This is shown in figure 4.13 on page 41.

As described in section 2.3 on page 17, the localization system uses short-time Fourier transform (STFT). The STFT uses a Hamming window to cut out chunks of the signal. Each chunk overlaps the preceding one with 50%, these chunks is then Fourier transformed (see (2.11) on page 18). This results in a representation of the signal in both time and frequency.

By applying a mask to the STFT and cut out the parts with insignificant energy, the number of samples needed to be sent for estimating TDOA can be greatly reduced. This is referred to as time-frequency masking (TFM). The compression ratio can be adjusted by varying the number of elements in the mask.

Compared to choosing the frequency components based on a time average of the whole signal, e.g. zonal sampling in section 4.2.2 on the facing page, this method gives the possibility to cut out different frequency components in different parts of the signal. This is a great advantage when localization is done on signals with an energy distribution in frequency that vary over time, such as the speech signal shown in figure 4.12 on page 41. However, in signals such as the 4-PSK in figure 4.13 on page 41 the advantage is not as great.

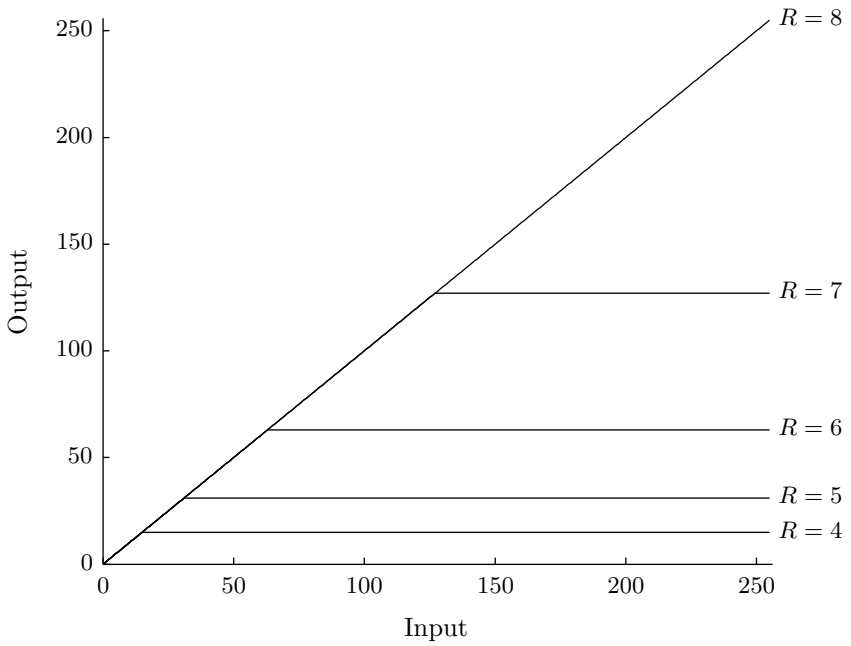

Figure 4.11: Output of the amplitude quantifier where $R_{\mathrm{MAX}} = 8$. Each line corresponds to the output for different assigned bits R.

4.3 Entropy Coding

Entropy coding, such as Huffman coding, is a lossless compression scheme and gives relatively little compression when compared to the lossy transform-quantization scheme. Furthermore, since it is lossless, it has no impact on localization performance, which makes it less interesting to simulate and measure.

An otherwise complete compression scheme for localization can be polished by entropy coding, but this thesis will not give entropy coding a thorough rundown.

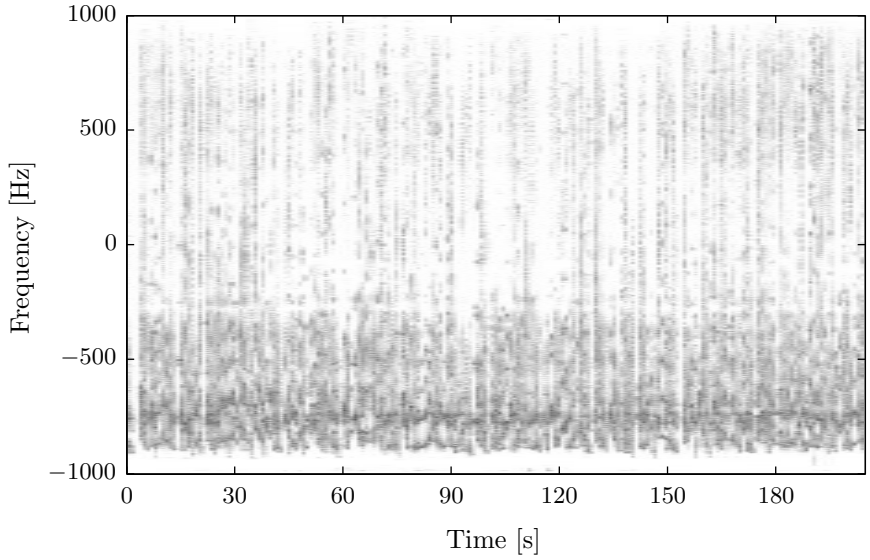

Figure 4.12: Spectrogram of a SSB speech signal. White is low energy and black is high energy.

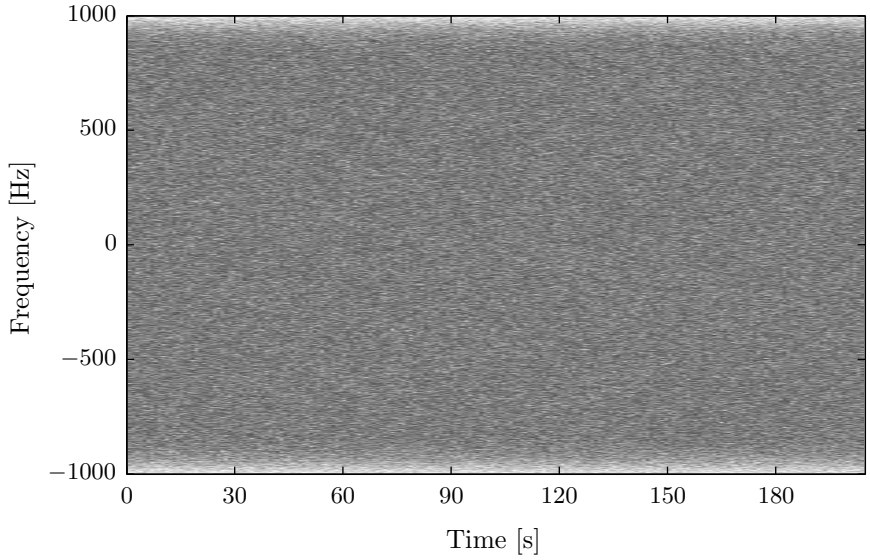

Figure 4.13: Spectrogram of a 4-PSK signal. White is low energy and black is high energy.

4.4 Distortion

This section adds the transform quantization noise to the SNR, and aims to provide a CRB for an optimal transform. The squared-error distortion,

$$D = E[(x - \hat{x})^2] \tag{4.7}$$

is a common measurement of the error introduced by quantization[4]. This is also comparable to the signal power. For a zero mean Gaussian source with variance σ^2, the rate distortion function, the given data rate R (in bits per sample) acheivable for a given distortion D, is

$$R(D) = \begin{cases} \frac{1}{2}\log_2 \frac{\sigma^2}{D} & 0 \leq D \leq \sigma^2 \\ 0, & D > \sigma^2 \end{cases} \tag{4.8}$$

which mean that we can express the distortion in terms of the rate as

$$D(R) = \sigma^2 2^{-2R}. \tag{4.9}$$

for an optimal quantization process[5]. For proofs and further details, see (Cover & Thomas, 2006, chapter 10). Assuming optimal quantization, for KLT, the decorrelation-optimal transform, the distortion is (Jayant & Noll, 1984, chapter 12)

$$D = (\det R_x)^{1/N} \cdot 2^{-2R}. \tag{4.10}$$

the SNR introduced by the KLT at rate R is

$$10 \log \frac{P_s}{D} = 10 \log \frac{P_s}{(\det R_x)^{1/N} \cdot 2^{-2R}} \tag{4.11}$$

The correlation matrix for $x = s + \nu$,

$$\begin{aligned} R_x &= E[(s+\nu)(s+\nu)^*] \\ &= E[(s+\nu)(s^*+\nu^*)] \\ &= E[ss^* + \nu s^* + s\nu^* + \nu\nu^*] \\ &= E[ss^*] + E[\nu s^*] + E[s\nu^*] + E[\nu\nu^*] \\ &\quad \big/ s \text{ and } \nu \text{ are independent} \big/ \\ &= E[ss^*] + 0 + 0 + E[\nu\nu^*] \\ &= R_s + R_\nu. \end{aligned} \tag{4.12}$$

Using a FSS signal scaled to let x have a gain SNR of σ^2, the signal s has power $P_s = \sigma^2$. The auto-correlation for the signal is then $R_s = \sigma^2$, and for noise with power $E_\nu = 1$, the auto-correlation matrix is $R_\nu = I$. The expression then becomes

$$R_x = (\sigma^2 + 1)I \tag{4.13}$$

Modelling the transfom as an additive guassian channel depicted in figure 4.14 on the facing page (Sayood, 2005, chapter 9), the added quantization

[4]This distortion is not the only alternative. For more information, see (Cover & Thomas, 2006, chapter 10).

[5]See equation (4.6) on page 38

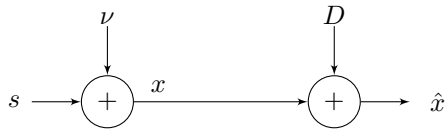

Figure 4.14: Gaussian channel with added quantization distortion.

noise is the distortion

$$\begin{aligned} D &= (\det R_x)^{1/N} \cdot 2^{-2R} \\ &= \left(\det((\sigma^2+1)I)\right)^{1/N} \cdot 2^{-2R} \\ &= \left((\sigma^2+1)^N\right)^{1/N} \cdot 2^{-2R} \\ &= (\sigma^2+1) \cdot 2^{-2R} \end{aligned} \tag{4.14}$$

so the SNR for the transform coded signal is

$$\text{SNR} = 10\log_{10}\left(\frac{P_s}{P_\nu + D}\right) = 10\log_{10}\left(\frac{\sigma^2}{1+(\sigma^2+1)\cdot 2^{-2R}}\right). \tag{4.15}$$

Reiterating the FIM, previously found as (2.19) on page 20,

$$\mathbf{J} = \frac{NB^2}{6} \cdot \frac{(\text{SNR})^2}{1+M\cdot(\text{SNR})} \cdot \frac{1}{c^2} \cdot \mathbf{G}\mathbf{G}^T, \tag{4.16}$$

the new SNR gain can be inserted

$$\begin{aligned} \mathbf{J} &= \frac{NB^2}{6} \cdot \frac{\left(\frac{\sigma^2}{1+(\sigma^2+1)\cdot 2^{-2R}}\right)^2}{1+M\cdot\left(\frac{\sigma^2}{1+(\sigma^2+1)\cdot 2^{-2R}}\right)} \cdot \frac{1}{c^2} \cdot \mathbf{G}\mathbf{G}^T \\ &= \frac{NB^2}{6} \cdot \frac{\sigma^4}{\left(1+(\sigma^2+1)\cdot 2^{-2R}\right)^2 + M\sigma^2\left(1+(\sigma^2+1)\cdot 2^{-2R}\right)} \cdot \frac{1}{c^2} \cdot \mathbf{G}\mathbf{G}^T \end{aligned} \tag{4.17}$$

Figure 4.15 on the following page depicts the impact of diffrent data rates per SNR level.

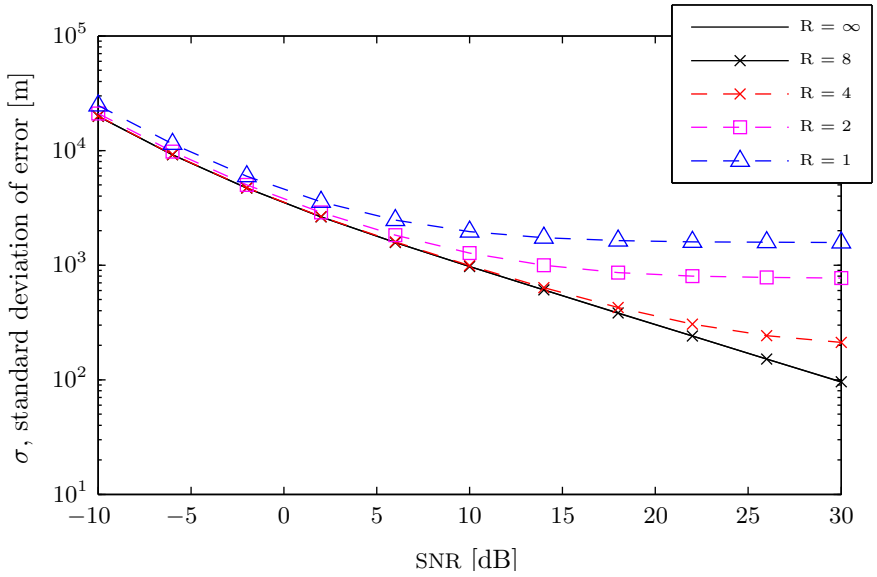

Figure 4.15: Cramér-Rao bound for a 1 s, 1 kHz flat spectrum signal, using different data rates R. Note that $R = 8$ and $R = \infty$ overlaps since $2^{-2 \cdot 8} \ll 1$ and have little impact on localization performance.

5 Evaulation by simulation

5.1 Experiment Setup

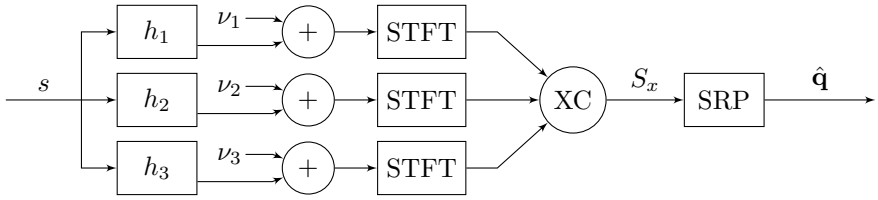

Figure 5.1: Localization system using TDOA and cross correlation.

The setup described in section 2.3 is used as a test bench for simulations to evaluate the compression techniques' impact on localization performance. The test bench is implemented in MATLAB.

Each signal is added with uncorrelated noise with different energy to test the performance of compression at different levels of SNR, see section 3.1 on page 23. The test is performed 100 times in order to determine the variance and mean of the localization error. The data is presented together with the CRB for FSSs (see section 2.4 on page 20).

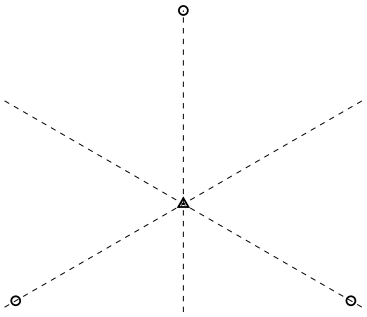

Figure 5.2: Experiment setup displaying the three receivers as circles and the transmitter as a triangle. The distance between the transmitter and receivers are $\sqrt{3} \cdot 10$ km and the receivers are evenly distributed around the transmitter forming a circle.

Figures show the standard deviation of the error as a function of SNR. The simulations setup gives an x and y symmetrical error due to the symmetrical node setup, see figure 5.2. Therefore, the figures in this chapter will show the standard deviation for a combined x and y data set.

The mean error is not shown in the figures, it is low compared to the standard deviation. Furthermore it will approach zero when the number of iterations is increased.

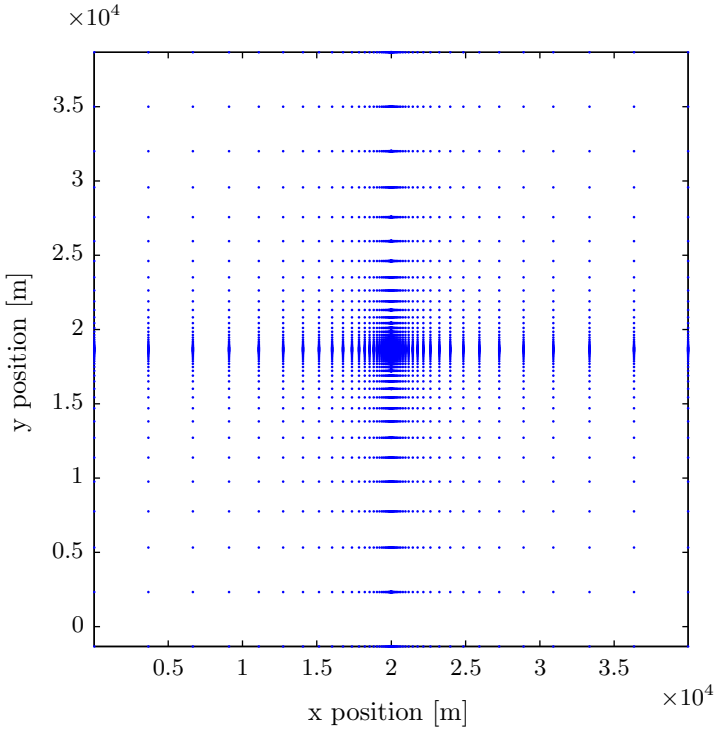

Figure 5.3: The logarithmic grid used for SRP calculations, with distances in meters. Each dot represent a position **u** used to calculate the SRP.

5.1.1 SRP Grid Granularity

To find the SRP peak described in equation 2.14 on page 18, we use a 100×100 grid, for positions **u**, as seen in figure 5.3. This grid is constructed to provide a fine grained resolution around the actual transmitter, so that the localization error due to the grid distance is proportional to the error. For implementation purposes, both x and y axis symmetry is needed.

There are other methods for finding the maximum SRP value, see e.g.Dmochowski *et al.* (2007), but the grid solution is easy to implement and good enough for this application. However, the grid (along with the sensor setup), makes it hard to measure errors of large magnitudes. The algorithm used will always find a maximum in one of the grid points, so errors larger than about 10^4 meters could be omitted, this should be taken into consideration when interpreting graphs.

5.1.2 Data Rate Reference

Complex data is generated as doubles in MATLAB, but both magnitude and phase data is quantized to 256 levels to be stored in $2 \cdot 8$ bits integers. This data is used to compare with the compressed version and the compression ratio is calculated using the 8 bit data as reference. As can be seen in figure 5.4 on the facing page, this does not have a significant impact on the localization ability. A reduction to 4 bits does hurt the ability, so 8 bits seems fair to use as a benchmark level. See also figure 4.15 on page 44.

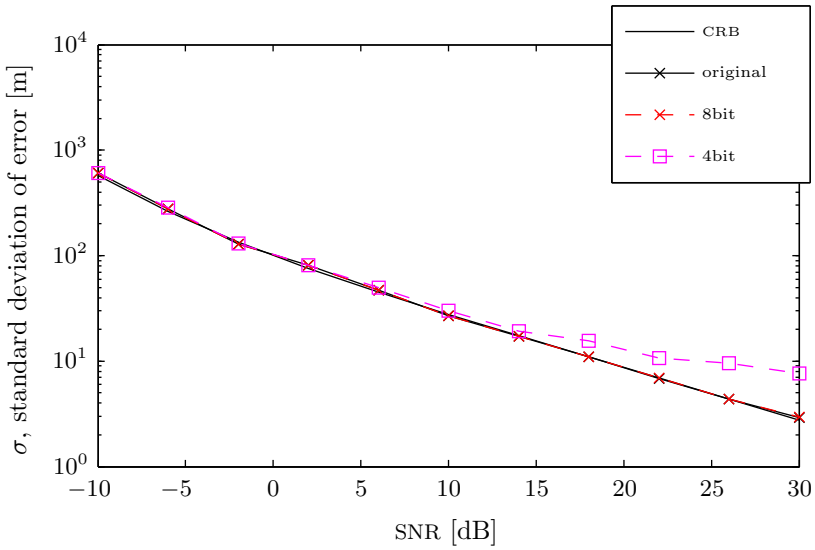

Figure 5.4: Comparison of the standard deviation of localization error at different SNR levels between CRB, uncompressed, 8 bit quantified, and 4 bit quantified FSS.

5.1.3 Block Effects

When analyzing the signal it is divided into blocks using a Hamming window with 50% overlap (as per 4.1.4 on page 31). Doing so doubles the number of blocks needed to be transmitted. The end blocks, containing only half a block of information and zero-padding, could be either kept or discarded, without noticeable results. In this thesis the end blocks is discarded.

A problem when using zero block overlap is block effects. The characteristics of the signal can change abruptly from one block to another. E.g in a speech signal one block may be a period of silence and the following block may be a voiced period. This will result in severe effects in the block transition and will affect localization. In the symmetrical simulation system used here, introducing block effects will have a positive impact on localization performance; the blocks themselves will correlate at $\Delta = 0$. Since this is specific to a symmetrical receiver array, this must be avoided in order to get a fair localization performance measurement of the compression schemes. Therefore a block overlap is preferred. The drawback of this is of course the increased data rate needed to transmit all the extra blocks. If these effects could be reduced or removed without block overlap, the compression ratio could be cut in half.

The block lengths used are 128 and 512. Different block lengths will affect the compression result, but these two are chosen to limit the degrees of freedom. Longer block lengths will give a more fine grained control over components in each block, but gives a more computationally complex algorithm and larger overhead. This is especially true for KLT based compression, but having the same block length for all algorithms increases comparability. The graphs and table data is based on block length $L_B = 512$ unless otherwise is stated.

5.1.4 Bandwidth and Signal Length

The bandwidth used is 2 kHz. The signal length is 303616 samples, chosen to give an approximate CRB of 100 meters at 0 dB SNR given the geometry used. The signal length is a quotient of the block length and gives $L = 4743$ blocks when using 50% overlap.

5.1.5 Compression Ratio

The ratio is calculated using $R = 2 \cdot 8$ bits per sample as reference. The block overlap, the type of transform used, and block length is information presumed to be predefined in the system, and thus unnecessary to transmit.

The total number of bits required by the compression scheme to represent and reconstruct the data is added together and divided with the total number of bits required to represent the uncompressed data,

$$\text{ratio} = \frac{\text{header} + \text{data}}{\text{original}}. \tag{5.1}$$

The header part is signal length independent, but the data is signal length dependent. In the sections below the ratio values for different transforms and compressions schemes are described, as well as example calculations.

5.1.5.1 KLT

The transform base components needed to reconstruct the data is stored. This gives a larger overhead compared to other transforms used in this thesis. With integer component quantization the data is paired with a bit vector with the same length as the block length L_B to represent which components that is discarded.

A calculation example can be done with block length $L_B = 128$, $K = 8$ components kept and signal length $L = 128000$. Using 50% block overlap this gives a total of 1999 blocks (throwing away the end blocks).

$$\text{header} = L_B + L_B \cdot K \cdot 16 \tag{5.2}$$

$$\text{data} = 1999 \cdot K \cdot 16 \tag{5.3}$$

$$\text{original} = 16 \cdot L \tag{5.4}$$

so

$$\text{ratio} = \frac{\text{header} + \text{data}}{\text{original}} = \frac{16512 + 255872}{2048000} \approx 0.1330 \tag{5.5}$$

The same parameters but with $K = 4$ components kept gives

$$\text{ratio} = \frac{\text{header} + \text{data}}{\text{original}} = \frac{8320 + 127936}{2048000} \approx 0.0665 \tag{5.6}$$

5.1.5.2 DFT and DCT

When using DFT or DCT the transform base components is unnecessary to transmit, since they are known given the block length. With integer component quantization the data is paired with a bit vector with the same length as the block to represent which components that are discarded. For partial components the data is paired with a bit vector of size $4 \cdot L_B$, where L_B is the block length. This bit vector describes the number of bits used for each transform component.

Using integer component quantization a calculation example can be done using $L_B = 128$ block length, $K = 8$ components kept and signal length $L = 128000$. Using 50% block overlap this gives a total of 1999 blocks (throwing away the end blocks).

$$\text{header} = L_B \tag{5.7}$$
$$\text{data} = 1999 \cdot K \cdot 16 \tag{5.8}$$
$$\text{original} = 16 \cdot L \tag{5.9}$$

so

$$\text{ratio} = \frac{\text{header} + \text{data}}{\text{original}} = \frac{128 + 255872}{2048000} = 0.1250 \tag{5.10}$$

The same parameters but with $K = 4$ components kept gives

$$\text{ratio} = \frac{\text{header} + \text{data}}{\text{original}} = \frac{128 + 127936}{2048000} \approx 0.0625 \tag{5.11}$$

Using partial components quantization a calculation example can be done using $L_B = 128$ block length, $R = 2 \cdot 4$ bits per sample on average and signal length $L = 128000$. Using 50% block overlap this gives a total of 1999 blocks (throwing away the end blocks).

$$\text{header} = 4 \cdot L_B \tag{5.12}$$
$$\text{data} = 1999 \cdot L_B \cdot R \tag{5.13}$$
$$\text{original} = 16 \cdot L \tag{5.14}$$

so

$$\text{ratio} = \frac{\text{header} + \text{data}}{\text{original}} = \frac{512 + 2046976}{2048000} \approx 0.9975 \tag{5.15}$$

The same parameters but with $R = 2 \cdot 2$ bits per sample on average gives

$$\text{ratio} = \frac{\text{header} + \text{data}}{\text{original}} = \frac{512 + 1023488}{2048000} \approx 0.5 \tag{5.16}$$

5.1.5.3 Time-Frequency Masking

When using time-frequency masking each block is paired with a vector with the same length as the block. The vector describes which components that is discarded and is necessary to reconstruct the signal. Since this information is paired with each block, no signal header is needed.

A calculation example can be done using $L_B = 128$ block length, signal length 128000, and 90% of the energy thrown away. For a FSS this gives approximately 10000 samples kept. Using 50% block overlap this gives a total of 1999 blocks (throwing away the end blocks).

$$\text{header} = 0 \tag{5.17}$$
$$\text{data} = \text{block header} + \text{actual data} = 1999 \cdot L_B + 10000 \cdot 16 \tag{5.18}$$
$$\text{original} = 16 \cdot L \tag{5.19}$$

so

$$\text{ratio} = \frac{\text{header} + \text{data}}{\text{original}} = \frac{0 + (255872 + 160000)}{2048000} \approx 0.203 \tag{5.20}$$

The same parameters but with 95% of the energy thrown gives approximately 5000 samples kept.

$$\text{ratio} = \frac{\text{header} + \text{data}}{\text{original}} = \frac{0 + (255872 + 80000)}{2048000} \approx 0.164 \tag{5.21}$$

5.1.6 Localization Ability Adjusted Compression Ratio

Another interesting measure of compression performance is to multiply the ratio with the (probably) decreased localization ability ratio. The motivation for this is found in the time proportional CRB variance; twice the standard deviation can be compensated by four times the signal length (see section 2.4 on page 20). This gives a localization ability adjusted ratio of

$$\text{adjusted ratio} = \frac{\text{header} + \text{data} \cdot \left(\sigma_{\text{compressed}}/\sigma_{\text{original}}\right)^2}{\text{original}}. \tag{5.22}$$

This is only precise for signals that does not vary in distribution over time, but is rather fair for signals that do not change dramatically.

An adjusted ratio value of above 1 means that the compression scheme reduced the localization ability more than it reduced the data. A value below 1 is a successful compression.

5.2 Evaluation of Compression Impact

The CRB used is for FSSs of similar bandwidth, regardless of the other signal types illustrated.

The signals used (FSS, 8-PSK, and SSB signals) are described in section 3.3 on page 24. Signals of each type with bandwidth 2 kHz were generated and three different WGN signals were added. The simulation was done 100 times per signal and SNR level. The PSK signals have deterministic maximum length sequence contents, the FSS are randomized each time and the SSB signals comes from different time chunks from the same audio book.

The only transform types used in simulations are KLT and DFT. The DCT is omitted since the signals are complex valued, and the DCT is optimized for real signals. Some early simulations were done using DCT, but they did not seem to diverge from the DFT case enough to merit further studies.

KLT is only used on the integral component quantization scheme, since it would carry a large overhead for other types of quantization.

The ratio value tables comes in pairs, the ratio achieved for a given simulation (an average over the iterations) and the localization ability adjusted ratio described in section 5.1.6. A ratio below 1 is a compression, a value above 1 is a data expansion, i.e., a lower value is better.

5.2.1 Compression Using Integral DFT Components

Here, we keep K components out of 512 in each block, based on the average signal energy in each block.

With the limitations of the grid mentioned in section 5.1.1 on page 46, effectively capping the possible error, figure 5.5 on the next page shows that keeping integral components is rather useless, since the nodes have a hard time separating the signal from the noise. Table 5.1 on page 52 further clarifies this, with ratio values over 1 for all SNR and numbers of components kept. See also section 4.2.1.1 on page 34 and 7.1.1 on page 89 for further discussion of this phenomenon.

For this type of compression, FSS and PSK behaves similarly, which can be seen in figure 5.6 on the next page and table 5.2 on page 52. The same conclusion is valid here, keeping integral components seems useless for noise-like signals, when no communication between the nodes are allowed.

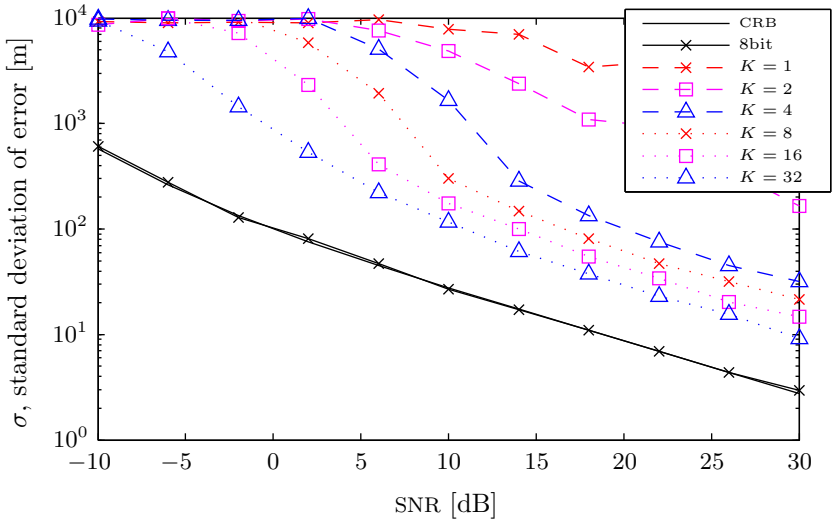

Figure 5.5: The standard deviation of the localization error using flat spectrum signals and keeping K integral DFT components.

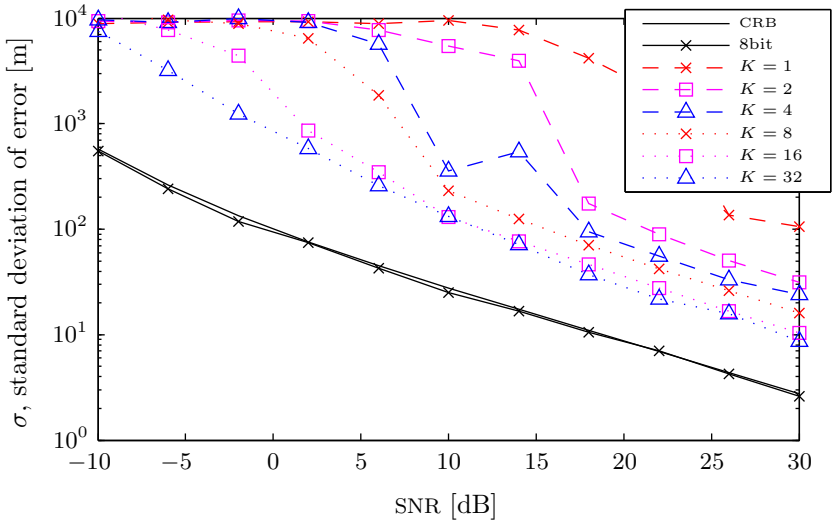

Figure 5.6: The standard deviation of the localization error using 8-PSK signals and keeping K integral DFT components.

SNR	8bit	$K = 1$	$K = 2$	$K = 4$	$K = 8$	$K = 16$	$K = 32$
all	1.00	0.00	0.01	0.02	0.03	0.06	0.12

(a) Ratio.

SNR	8bit	$K = 1$	$K = 2$	$K = 4$	$K = 8$	$K = 16$	$K = 32$
−10	1.00	0.90	1.55	3.98	13.55	23.04	29.68
−6	1.00	4.12	10.19	18.69	44.48	81.08	37.46
−2	1.00	19.51	41.31	85.32	192.33	192.61	15.46
2	1.00	47.76	112.43	232.49	163.24	51.15	5.51
6	1.00	166.42	204.54	185.65	53.76	4.80	2.83
10	1.00	328.14	256.03	59.18	3.89	2.67	2.34
14	1.00	646.80	152.31	4.32	2.32	2.12	1.63
18	1.00	379.27	76.32	2.31	1.69	1.54	1.45
22	1.00	1190.14	140.57	1.86	1.42	1.48	1.36
26	1.00	633.86	53.28	1.66	1.65	1.38	1.59
30	1.00	328.07	25.08	1.83	1.66	1.56	1.23

(b) Adjusted ratio.

Table 5.1: Ratio calculations when keeping K integral DFT components for flat spectrum signals.

SNR	8bit	$K = 1$	$K = 2$	$K = 4$	$K = 8$	$K = 16$	$K = 32$
all	1.00	0.00	0.01	0.02	0.03	0.06	0.12

(a) Ratio.

SNR	8bit	$K = 1$	$K = 2$	$K = 4$	$K = 8$	$K = 16$	$K = 32$
−10	1.00	1.01	2.26	4.75	12.98	26.59	23.43
−6	1.00	5.67	11.33	22.72	50.13	63.66	21.82
−2	1.00	24.02	50.66	109.92	176.58	88.00	13.96
2	1.00	59.60	124.12	232.94	234.56	8.41	7.54
6	1.00	167.60	252.68	273.84	58.62	4.13	4.51
10	1.00	556.28	366.76	3.20	2.69	1.69	3.47
14	1.00	829.72	435.61	16.29	1.72	1.29	2.25
18	1.00	613.29	2.14	1.26	1.41	1.21	1.52
22	1.00	291.07	1.27	0.98	1.12	0.99	1.21
26	1.00	4.03	1.11	0.95	1.16	0.97	1.70
30	1.00	6.35	1.10	1.30	1.18	0.99	1.35

(b) Adjusted ratio.

Table 5.2: Ratio calculations when keeping K integral DFT components for 8-PSK signals.

For SSB, which differs from the noise, more interesting things appear. As seen in figure 5.7 on the next page, the localization ability follows that of the 8bits signal. Combining this with the ratio values seen in table 5.3a on page 54, we get the localization ability adjusted ratio values of table 5.3b on page 54. With numbers below 1 for SNRs below ~ 20 dB, indicating a data compression. This is a positive result. This holds for most of the numbers of components kept, but $K = 2$ or $K = 4$ delivers best results.

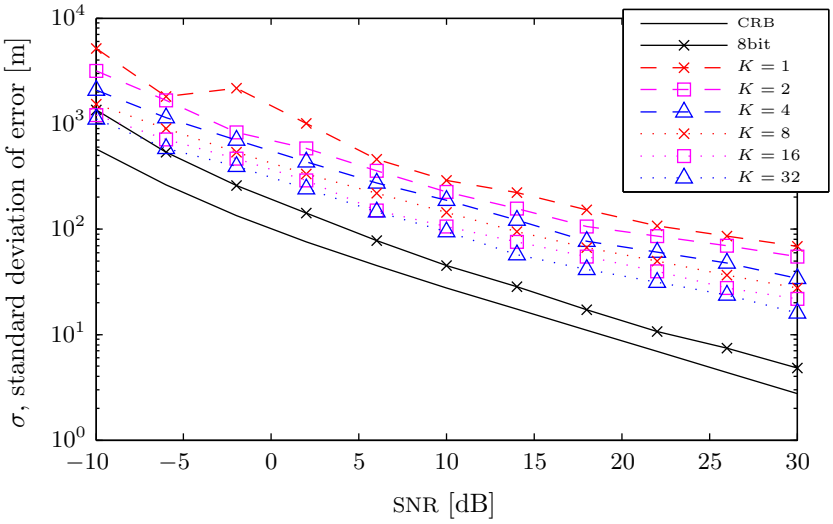

Figure 5.7: The standard deviation of the localization error using SSB signals and keeping K integral DFT components.

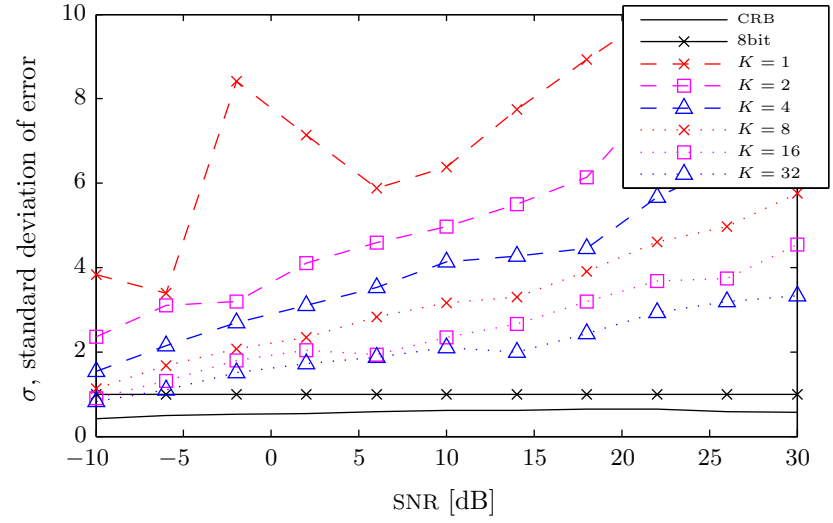

Figure 5.8: The quotient of the standard deviation of the localization error for SSB signals using 8 bit as reference. Each line corresponds to keeping K integral DFT components. If the y axis value is 2, the σ is two times that of the 8 bit signal.

SNR	8bit	$K=1$	$K=2$	$K=4$	$K=8$	$K=16$	$K=32$
all	1.00	0.00	0.01	0.02	0.03	0.06	0.12

(a) Ratio.

SNR	8bit	$K=1$	$K=2$	$K=4$	$K=8$	$K=16$	$K=32$
−10	1.00	0.06	0.04	0.04	0.04	0.05	0.08
−6	1.00	0.05	0.08	0.07	0.09	0.11	0.15
−2	1.00	0.28	0.08	0.11	0.13	0.20	0.29
2	1.00	0.20	0.13	0.15	0.17	0.26	0.37
6	1.00	0.14	0.17	0.19	0.25	0.23	0.44
10	1.00	0.16	0.19	0.27	0.31	0.34	0.55
14	1.00	0.23	0.24	0.28	0.34	0.44	0.50
18	1.00	0.31	0.29	0.31	0.48	0.63	0.74
22	1.00	0.39	0.50	0.50	0.66	0.85	1.07
26	1.00	0.53	0.69	0.65	0.77	0.87	1.28
30	1.00	0.81	1.03	0.78	1.03	1.29	1.38

(b) Adjusted ratio.

Table 5.3: Ratio calculations when keeping K integral DFT components for single side band signals.

5.2.2 Compression Using Integral KLT Components

Switching transform method to the KLT and comparing figure 5.9 on the facing page for KLT and figure 5.5 on page 51 for DFT, there are noticeable difference. The KLT performs more evenly along the SNR values, beating the DFT for weak signals and the opposite for strong signals.

The ratio calculations differs, table 5.4a on the facing page indicates about 50% larger overhead than its DFT counterpart, resulting in worse ratio values for those K-SNR combinations with lower ratio values. Where DFT performs abhorrently bad[1], the KLT performs better, but fails to get below 1.

8-PSK tells the same story; KLT performs more evenly, but still bad.

For SSB signals, the KLT captures the signal properties well, giving an adjusted ratio under 1 for all SNR levels and all K numbers[2] of components saved.

[1] Ratio values of over 100, indicating a required data rate of above 100 times the original rate for the same localization ability. This can not be called compression at all.

[2] Of those simulated.

SNR	8bit	$K=1$	$K=2$	$K=4$	$K=8$	$K=16$	$K=32$
all	1.00	0.01	0.01	0.02	0.04	0.09	0.18

(a) Ratio.

SNR	8bit	$K=1$	$K=2$	$K=4$	$K=8$	$K=16$	$K=32$
−10	1.00	2.57	4.77	7.95	7.46	3.24	1.97
−6	1.00	11.51	18.86	21.32	9.06	3.41	1.93
−2	1.00	51.03	60.20	36.68	12.87	6.30	3.00
2	1.00	94.13	58.00	28.85	9.88	7.65	3.79
6	1.00	156.37	44.98	28.75	13.82	9.89	4.88
10	1.00	141.76	46.93	26.07	20.68	12.13	6.33
14	1.00	85.82	44.52	29.07	20.27	12.84	8.42
18	1.00	53.38	45.61	26.94	22.16	17.41	9.40
22	1.00	52.80	54.96	37.91	31.73	21.59	11.78
26	1.00	51.43	57.11	45.47	32.18	23.05	15.90
30	1.00	42.22	54.42	45.76	33.68	24.01	17.04

(b) Adjusted ratio.

Table 5.4: Ratio calculations when keeping K integral KLT components for flat spectrum signals.

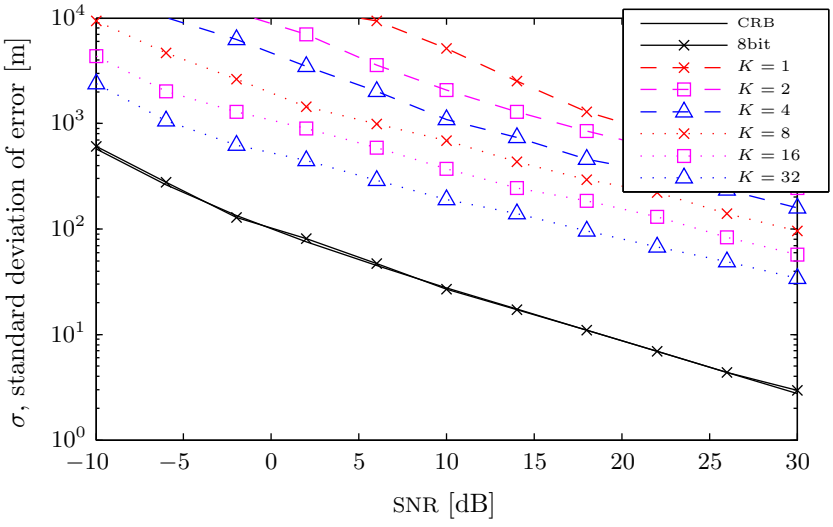

Figure 5.9: The standard deviation of the localization error using flat spectrum signals and keeping K integral KLT components.

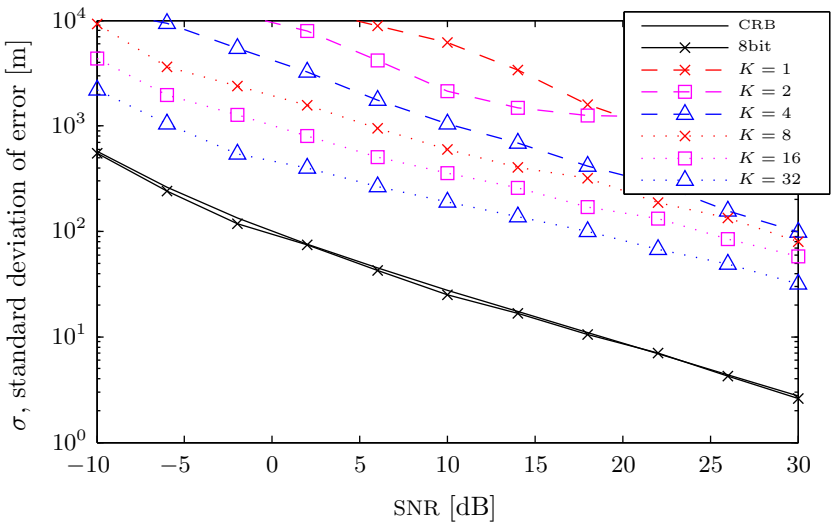

Figure 5.10: The standard deviation of the localization error using 8-PSK signals and keeping K integral KLT components.

SNR	8bit	$K = 1$	$K = 2$	$K = 4$	$K = 8$	$K = 16$	$K = 32$
all	1.00	0.01	0.01	0.02	0.04	0.09	0.18

(a) Ratio.

SNR	8bit	$K = 1$	$K = 2$	$K = 4$	$K = 8$	$K = 16$	$K = 32$
−10	1.00	3.25	6.03	8.55	8.74	3.93	2.05
−6	1.00	16.01	22.53	23.94	7.14	4.17	2.41
−2	1.00	61.82	77.21	33.21	12.69	7.24	2.70
2	1.00	125.48	87.62	29.80	13.71	7.35	3.58
6	1.00	166.60	74.25	26.33	15.38	8.80	4.83
10	1.00	239.48	57.24	26.90	17.77	12.69	7.19
14	1.00	157.16	60.51	25.96	18.14	14.64	8.39
18	1.00	88.85	111.87	24.08	28.74	16.18	11.18
22	1.00	68.99	234.65	25.30	22.43	22.16	11.59
26	1.00	73.37	436.85	21.00	31.33	24.35	16.47
30	1.00	77.60	1007.08	21.86	29.36	30.28	18.57

(b) Adjusted ratio.

Table 5.5: Ratio calculations when keeping K integral KLT components for 8-PSK signals.

SNR	8bit	$K = 1$	$K = 2$	$K = 4$	$K = 8$	$K = 16$	$K = 32$
all	1.00	0.01	0.01	0.02	0.04	0.09	0.18

(a) Ratio.

SNR	8bit	$K = 1$	$K = 2$	$K = 4$	$K = 8$	$K = 16$	$K = 32$
-10	1.00	0.09	0.05	0.07	0.14	0.23	0.37
-6	1.00	0.11	0.07	0.10	0.13	0.23	0.33
-2	1.00	0.10	0.09	0.12	0.19	0.27	0.34
2	1.00	0.14	0.11	0.12	0.20	0.29	0.37
6	1.00	0.15	0.15	0.17	0.27	0.49	0.51
10	1.00	0.18	0.15	0.24	0.48	0.52	0.60
14	1.00	0.16	0.17	0.24	0.59	0.51	0.79
18	1.00	0.20	0.23	0.18	0.64	0.58	0.79
22	1.00	0.21	0.22	0.23	0.54	0.70	0.96
26	1.00	0.18	0.16	0.19	0.42	0.53	0.78
30	1.00	0.17	0.15	0.18	0.40	0.50	0.96

(b) Adjusted ratio.

Table 5.6: Ratio calculations when keeping K integral KLT components for single side band signals.

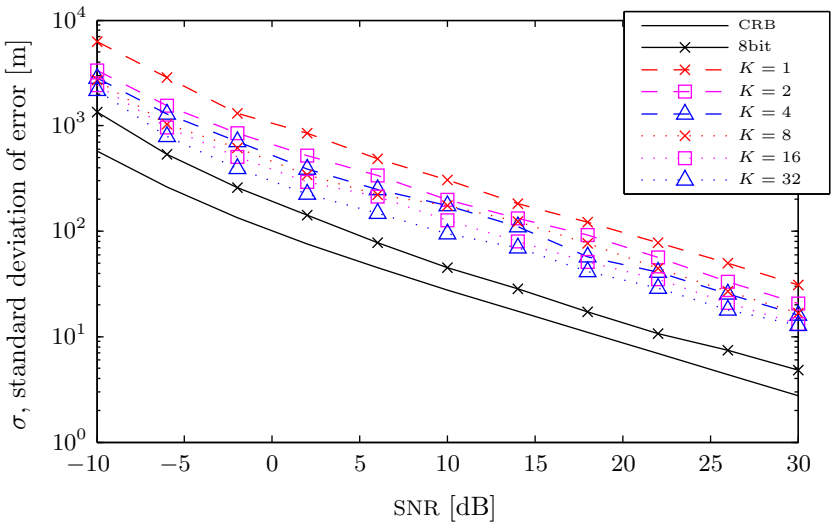

Figure 5.11: The standard deviation of the localization error using SSB signals and keeping K integral KLT components.

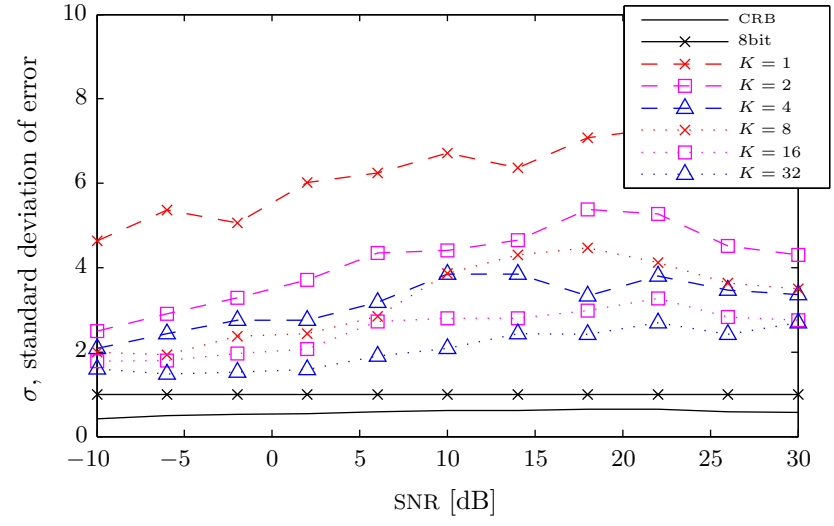

Figure 5.12: The quotient of the standard deviation of the localization error for SSB signals using 8 bit as reference. Each line corresponds to keeping K integral KLT components. If the y axis value is 2, the σ is two times that of the 8 bit signal.

5.2.3 Compression Using Partial Components

For figures showing the partial component scheme, "$R = 4$" should be interpreted as $R = 2 \cdot 4$ bits per component *on average*. This is consistent with the "8bit" notation for the reference signals. Here, the same number of bits are assigned to the magnitude and the phase data for each component.

The first interesting result here is that the figures are strikingly similar for both FSS, 8-PSK and SSB signals, see figures 5.13 to 5.15 on pages 61–62. The second promising finding is that for 2 bits on average, the localization ability adjusted ratio is below 1 for all signals with 2 dB SNR or lower, see tables 5.7b, 5.9b, and 5.8b. The specific scheme we use, described in section 4.2.2 on page 38, fails for lower number of bits allocated than 2. This is thought to be due to the poor phase granularity at 1 bit components. If further data reduction is wanted, there should probably be a redistribution of bits from the amplitude data to the phase data.

SNR	8bit	R=2	R=4	R=6
all	1.00	0.50	1.00	1.50

(a) Ratio.

SNR	8bit	R=2	R=4	R=6
−10	1.00	0.65	0.85	1.24
−6	1.00	0.66	0.98	1.59
−2	1.00	0.92	1.14	1.53
2	1.00	0.56	0.98	1.14
6	1.00	0.87	1.13	1.54
10	1.00	1.07	1.29	1.67
14	1.00	1.36	1.67	1.77
18	1.00	1.53	2.34	1.99
22	1.00	2.50	2.69	2.08
26	1.00	4.30	4.53	2.22
30	1.00	5.58	7.13	2.84

(b) Adjusted ratio.

Table 5.7: Ratio calculations using partial components for flat spectrum signals.

SNR	8bit	R=2	R=4	R=6
all	1.00	0.50	1.00	1.50

(a) Ratio.

SNR	8bit	R=2	R=4	R=6
−10	1.00	0.74	0.86	1.30
−6	1.00	0.76	1.05	1.58
−2	1.00	0.97	1.24	1.96
2	1.00	0.63	1.00	1.59
6	1.00	0.72	1.11	1.72
10	1.00	1.45	1.44	1.90
14	1.00	1.67	1.22	1.50
18	1.00	2.48	2.10	1.92
22	1.00	3.13	2.97	1.71
26	1.00	5.11	3.76	1.90
30	1.00	8.83	6.70	2.85

(b) Adjusted ratio.

Table 5.8: Ratio calculations using partial components for 8-PSK signals.

SNR	8bit	R=2	R=4	R=6
all	1.00	0.50	1.00	1.50

(a) Ratio.

SNR	8bit	R=2	R=4	R=6
−10	1.00	0.92	1.08	1.52
−6	1.00	0.91	1.10	2.30
−2	1.00	0.82	1.19	1.56
2	1.00	0.78	1.16	1.43
6	1.00	1.02	1.21	1.40
10	1.00	1.07	1.13	1.61
14	1.00	1.43	1.38	1.67
18	1.00	1.71	1.72	1.72
22	1.00	1.77	2.28	2.16
26	1.00	3.44	2.19	2.64
30	1.00	4.19	2.92	3.12

(b) Adjusted ratio.

Table 5.9: Ratio calculations using partial components for single side band signals.

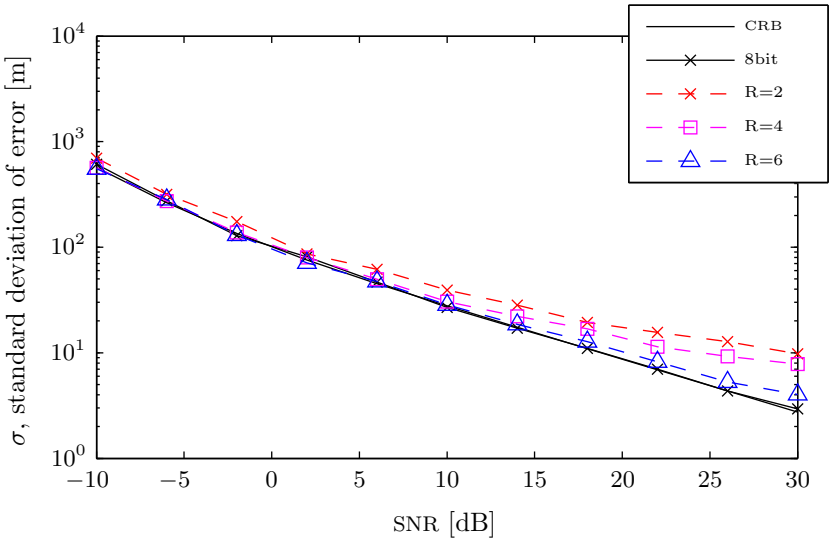

Figure 5.13: The standard deviation of the localization error using flat spectrum signals and keeping partial DFT components. Each line corresponds to different number of bits assigned.

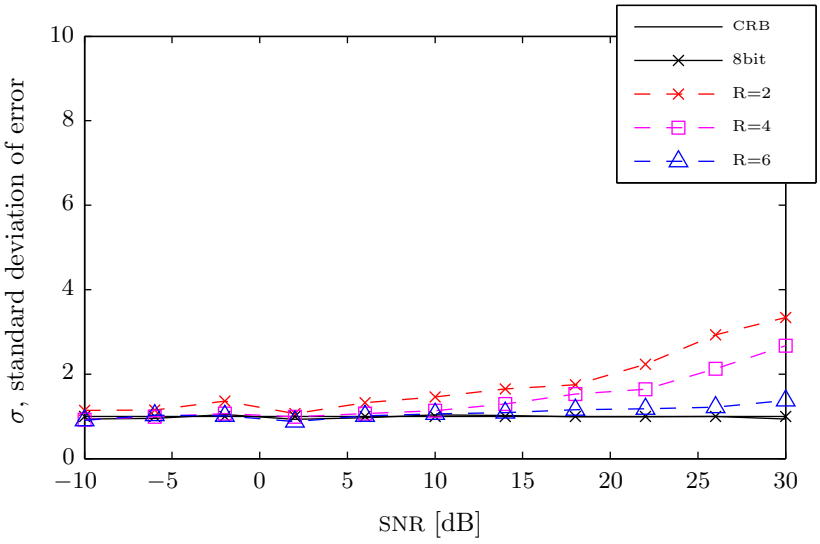

Figure 5.14: The quotient of the standard deviation of the localization error for flat spectrum signals and keeping partial DFT components. The figure use 8 bit as reference. Each line corresponds to different number of bits assigned. If the y axis value is 2, the σ is two times that of the 8 bit signal.

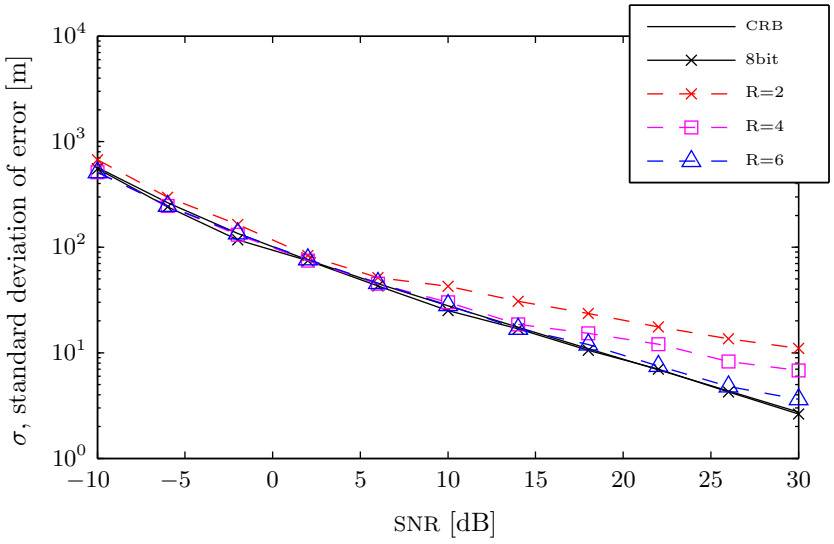

Figure 5.15: The standard deviation of the localization error using 8-PSK signals and keeping partial DFT components. Each line corresponds to different number of bits assigned.

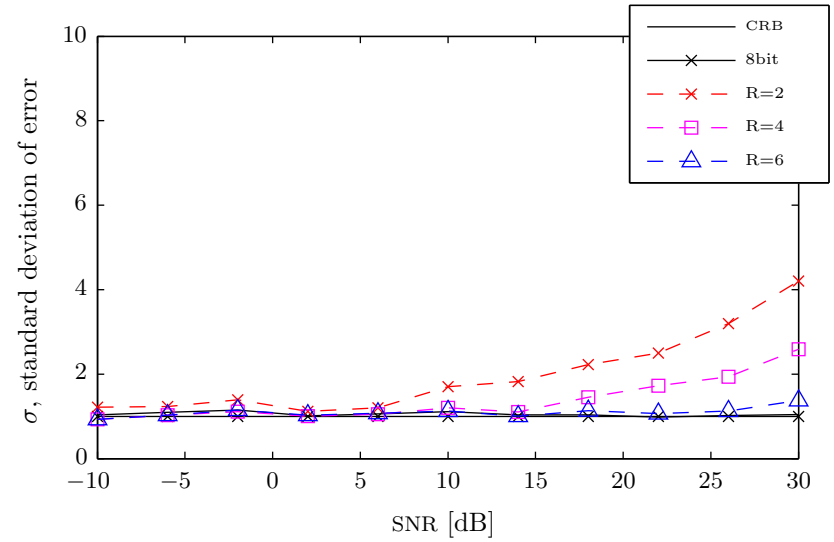

Figure 5.16: The quotient of the standard deviation of the localization error for 8-PSK signals and keeping partial DFT components using 8 bit as reference. Each line corresponds to different number of bits assigned. If the y axis value is 2, the σ is two times that of the 8 bit signal.

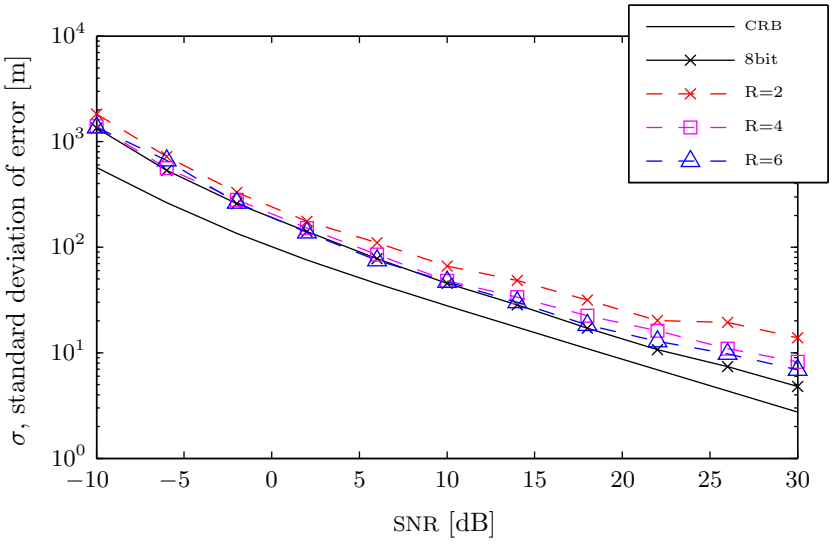

Figure 5.17: The standard deviation of the localization error using single side band signals and keeping partial DFT components. Each line corresponds to different number of bits assigned.

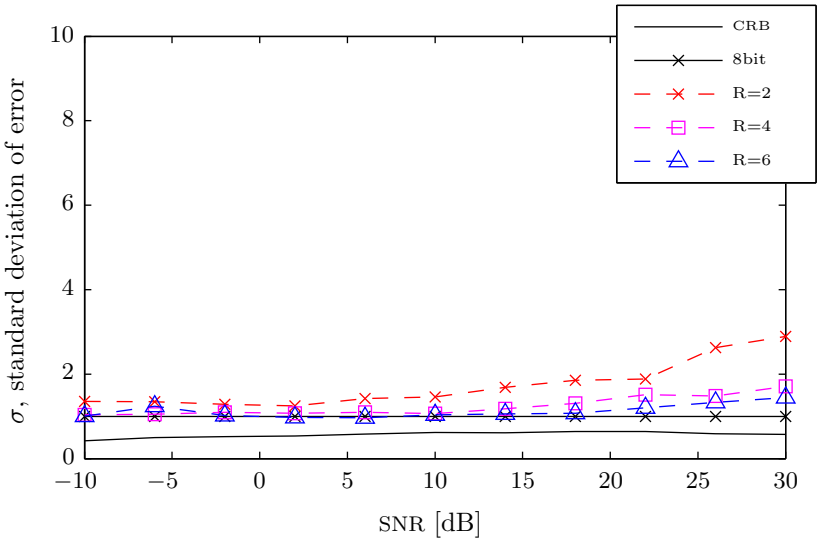

Figure 5.18: The quotient of the standard deviation of the localization error for single side band signals and keeping partial DFT components using 8 bit as reference. Each line corresponds to different number of bits assigned. If the y axis value is 2, the σ is two times that of the 8 bit signal.

5.2.4 Compression Using Time-Frequency Masking

For TFM, "70%" the interpretation should be "70% of the signal energy is cut". The trend for TFM on FSS follows the one for the uncompressed version (figure 5.19 on the facing page), but not closely enough (figure 5.20 on page 66) for it to achieve compression when the ratio is adjusted for the localization ability regression when a lot of the signal energy is cut. A slight compression is achieved for high SNR levels when cutting only a small part of the signal energy. (see table 5.10b).

Time-frequency DFT masking for 8-PSK behaves almost exactly as for FSS, compare the values of table 5.11 on the next page to those of table 5.10.

SNR	8bit	99%	95%	90%	80%	70%	60%	50%	40%	30%
−10	1.00	0.13	0.14	0.17	0.22	0.30	0.39	0.50	0.63	0.79
−6	1.00	0.13	0.14	0.17	0.22	0.30	0.39	0.50	0.63	0.79
−2	1.00	0.13	0.14	0.17	0.22	0.30	0.39	0.50	0.63	0.79
2	1.00	0.13	0.14	0.17	0.22	0.30	0.39	0.50	0.63	0.79
6	1.00	0.13	0.14	0.17	0.22	0.30	0.39	0.50	0.63	0.79
10	1.00	0.13	0.14	0.17	0.23	0.30	0.39	0.50	0.63	0.79
14	1.00	0.13	0.14	0.17	0.23	0.30	0.39	0.50	0.63	0.79
18	1.00	0.13	0.14	0.17	0.23	0.30	0.39	0.50	0.63	0.79
22	1.00	0.13	0.14	0.17	0.23	0.30	0.39	0.50	0.63	0.79
26	1.00	0.13	0.14	0.17	0.23	0.30	0.39	0.50	0.63	0.79
30	1.00	0.13	0.14	0.17	0.23	0.30	0.39	0.50	0.63	0.79

(a) Ratio.

SNR	8bit	99%	95%	90%	80%	70%	60%	50%	40%	30%
−10	1.00	76.84	30.33	9.41	2.45	1.73	1.33	0.94	0.99	1.07
−6	1.00	293.50	21.37	6.22	2.17	1.49	1.26	1.26	1.11	1.00
−2	1.00	181.11	14.37	4.72	2.24	1.60	1.38	1.09	1.09	1.26
2	1.00	44.01	4.70	2.35	1.40	1.23	1.11	1.11	1.07	1.05
6	1.00	21.33	3.43	1.88	1.28	0.95	1.06	0.86	1.01	1.03
10	1.00	15.03	3.01	1.73	1.09	0.99	0.92	0.94	0.98	1.19
14	1.00	10.70	2.59	1.26	0.90	0.84	0.78	0.95	0.88	1.34
18	1.00	7.68	2.24	1.24	1.00	0.80	0.89	1.03	1.04	0.96
22	1.00	8.44	1.83	1.09	0.74	0.78	0.57	0.90	0.94	0.99
26	1.00	11.71	2.18	1.42	1.09	0.72	0.66	0.84	0.90	0.94
30	1.00	11.01	2.07	1.34	0.92	0.93	0.85	0.86	0.91	0.84

(b) Adjusted ratio.

Table 5.10: Ratio calculations using TFM for flat spectrum signals. The percentages corresponds to the amount of energy thrown.

SNR	8bit	99%	95%	90%	80%	70%	60%	50%	40%	30%
−10	1.00	0.13	0.14	0.17	0.22	0.30	0.39	0.50	0.63	0.79
−6	1.00	0.13	0.14	0.17	0.22	0.30	0.39	0.50	0.63	0.79
−2	1.00	0.13	0.14	0.17	0.22	0.30	0.39	0.50	0.63	0.79
2	1.00	0.13	0.14	0.16	0.22	0.29	0.38	0.49	0.62	0.78
6	1.00	0.13	0.14	0.16	0.22	0.29	0.38	0.49	0.61	0.77
10	1.00	0.13	0.14	0.16	0.22	0.29	0.38	0.48	0.61	0.77
14	1.00	0.13	0.14	0.16	0.22	0.29	0.38	0.48	0.61	0.76
18	1.00	0.13	0.14	0.16	0.22	0.29	0.38	0.48	0.60	0.76
22	1.00	0.13	0.14	0.16	0.22	0.29	0.37	0.48	0.60	0.76
26	1.00	0.13	0.14	0.16	0.22	0.29	0.37	0.48	0.60	0.76
30	1.00	0.13	0.14	0.16	0.22	0.29	0.37	0.48	0.60	0.76

(a) Ratio.

SNR	8bit	99%	95%	90%	80%	70%	60%	50%	40%	30%
−10	1.00	89.19	40.91	6.47	2.84	1.48	1.36	1.06	1.03	1.04
−6	1.00	327.29	16.50	7.42	2.53	1.90	1.36	1.42	1.41	1.48
−2	1.00	148.63	12.67	4.02	2.17	1.82	1.50	1.38	1.61	1.34
2	1.00	35.67	4.79	2.17	1.24	1.13	1.07	0.85	1.06	1.03
6	1.00	18.90	3.81	1.46	1.22	1.08	1.00	0.91	1.00	1.01
10	1.00	12.97	3.26	1.70	1.07	1.08	0.81	0.97	1.07	1.09
14	1.00	10.09	2.28	1.25	0.94	0.84	0.73	0.86	0.85	1.03
18	1.00	8.89	1.87	1.19	0.81	0.69	0.85	0.73	0.96	0.82
22	1.00	6.56	1.90	0.98	0.70	0.64	0.76	0.75	0.69	0.80
26	1.00	9.19	2.23	0.98	0.89	0.70	0.74	0.75	0.86	1.10
30	1.00	11.74	2.66	1.45	0.98	0.82	0.94	0.90	1.05	1.02

(b) Adjusted ratio.

Table 5.11: Ratio calculations using TFM for 8-PSK signals. The percentage corresponds to the amount of energy thrown.

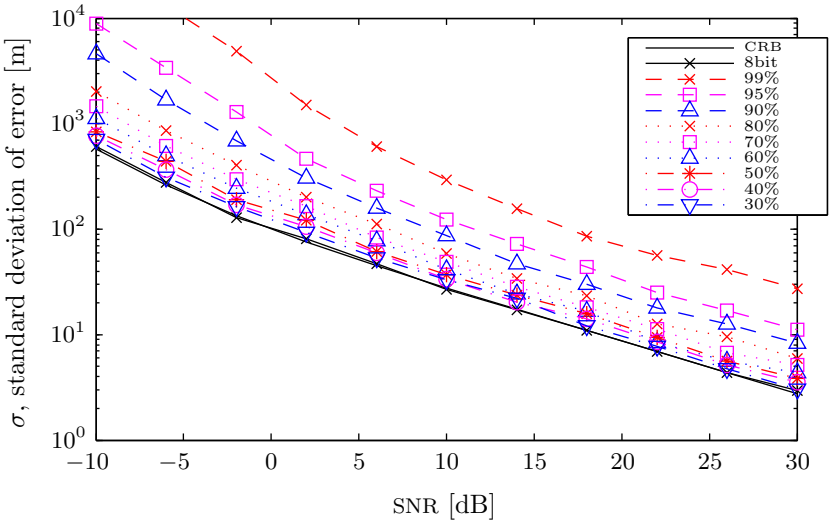

Figure 5.19: The standard deviation of the localization error using flat spectrum signals and time-frequency masking. The percentages corresponds to the amount of energy thrown.

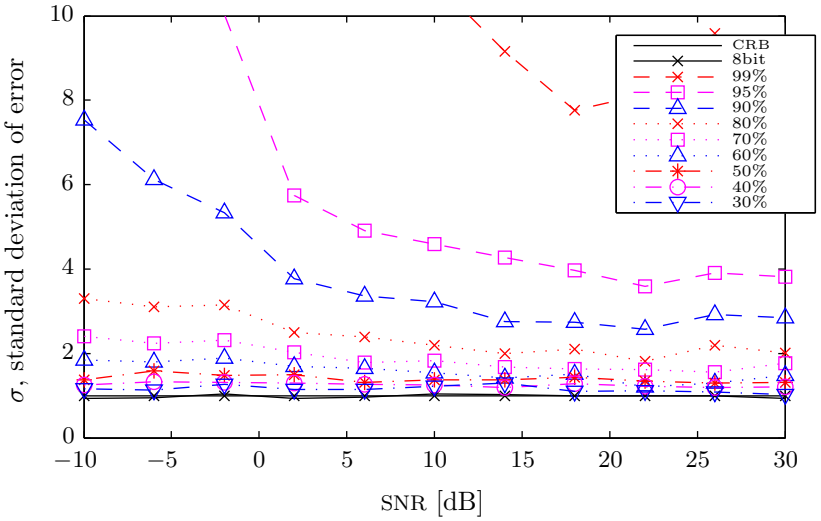

Figure 5.20: The quotient of the standard deviation of the localization error for flat spectrum signals and time-frequency masking, using 8 bit as reference. The percentages corresponds to the amount of energy thrown. If the y axis value is 2, the σ is two times that of the 8 bit signal.

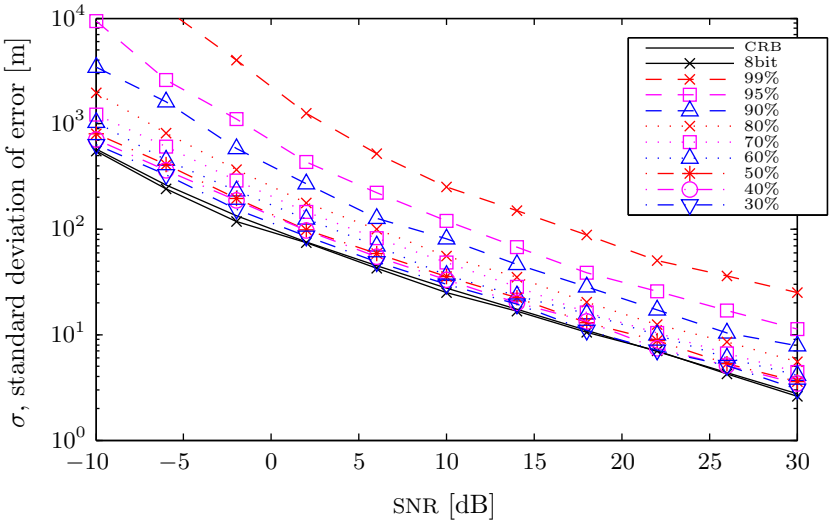

Figure 5.21: The standard deviation of the localization error using 8-PSK signals and time-frequency masking The percentages cores-ponds to the amount of energy thrown.

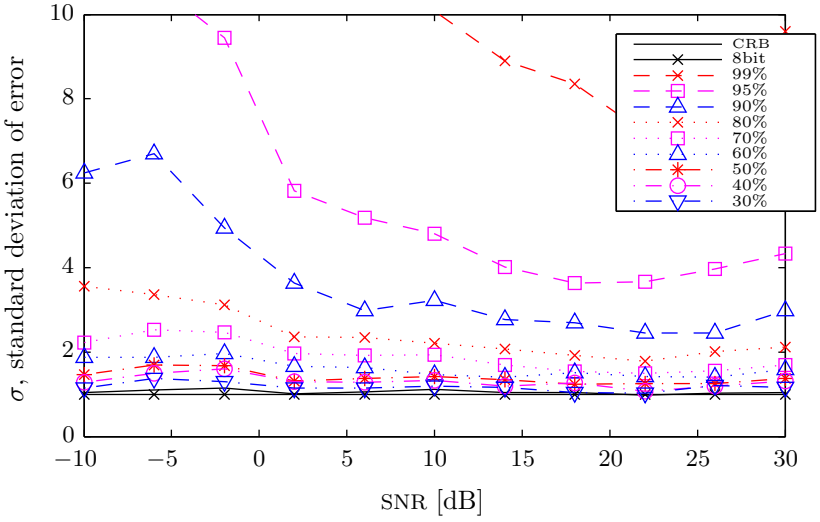

Figure 5.22: The quotient of the standard deviation of the localization error for 8-PSK signals and time-frequency masking, using 8 bit as reference. The percentage corresponds to the amount of energy thrown. If the y axis value is 2, the σ is two times that of the 8 bit signal.

For low SNR levels, TFM performs rather well for SSB signals. Here, the scheme removes a lot of noise, improving localization ability. Illustration in figures 5.23 to 5.24 on the next page. In table 5.12b, one can see that, interestingly enough, one should cut relatively little energy from the signal. Figures 5.23 to 5.24 on the next page show the performance of this scheme on SSB speech signals.

SNR	8bit	99%	95%	90%	80%	70%	60%	50%	40%	30%
−10	1.00	0.13	0.13	0.15	0.21	0.28	0.37	0.47	0.60	0.77
−6	1.00	0.13	0.13	0.14	0.17	0.23	0.32	0.42	0.55	0.71
−2	1.00	0.12	0.13	0.13	0.14	0.16	0.22	0.31	0.43	0.60
2	1.00	0.12	0.13	0.13	0.13	0.14	0.15	0.18	0.26	0.39
6	1.00	0.12	0.13	0.13	0.13	0.13	0.14	0.15	0.17	0.22
10	1.00	0.12	0.13	0.13	0.13	0.13	0.13	0.14	0.15	0.18
14	1.00	0.12	0.13	0.13	0.13	0.13	0.13	0.14	0.15	0.17
18	1.00	0.12	0.13	0.13	0.13	0.13	0.13	0.14	0.15	0.16
22	1.00	0.12	0.13	0.13	0.13	0.13	0.13	0.14	0.15	0.16
26	1.00	0.12	0.13	0.13	0.13	0.13	0.13	0.14	0.15	0.16
30	1.00	0.12	0.13	0.13	0.13	0.13	0.13	0.14	0.15	0.16

(a) Ratio.

SNR	8bit	99%	95%	90%	80%	70%	60%	50%	40%	30%
−10	1.00	0.28	0.07	0.06	0.09	0.10	0.18	0.25	0.38	0.53
−6	1.00	1.29	0.26	0.14	0.12	0.13	0.18	0.23	0.39	0.56
−2	1.00	4.30	0.94	0.53	0.22	0.14	0.16	0.19	0.34	0.47
2	1.00	7.28	1.33	0.78	0.47	0.27	0.24	0.20	0.19	0.28
6	1.00	17.36	2.82	1.58	0.67	0.53	0.48	0.34	0.27	0.27
10	1.00	27.74	4.00	2.32	1.18	0.59	0.50	0.48	0.29	0.34
14	1.00	36.21	6.24	2.91	1.15	0.95	0.62	0.43	0.41	0.36
18	1.00	59.24	8.83	4.48	2.04	0.99	0.76	0.65	0.45	0.43
22	1.00	100.35	17.22	8.24	3.28	2.05	1.37	0.77	0.72	0.51
26	1.00	156.10	18.73	10.42	3.93	2.00	1.30	0.79	0.72	0.57
30	1.00	222.69	32.83	13.43	5.65	3.68	2.03	1.28	1.08	0.76

(b) Adjusted ratio.

Table 5.12: Ratio calculations using time-frequency masking for single side band signals. The percentages corresponds to the amount of energy thrown.

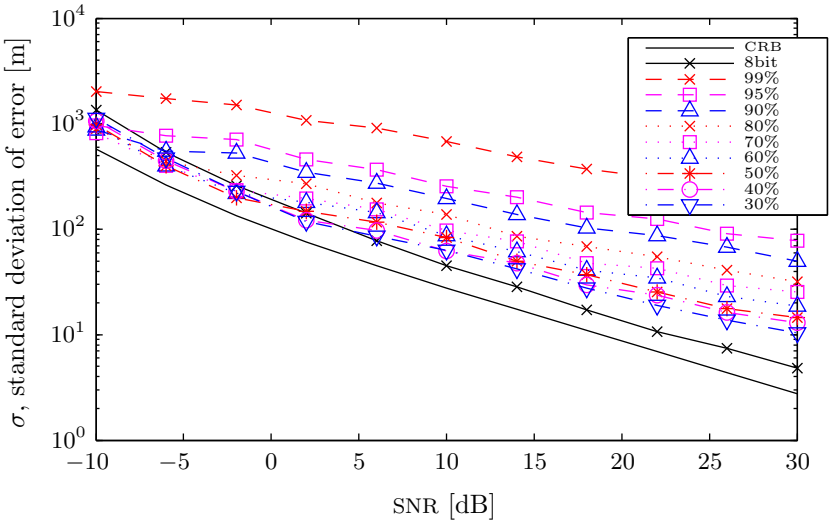

Figure 5.23: The standard deviation of the localization error using single side band signals and time-frequency masking. The percentage correspond to the amount of energy thrown.

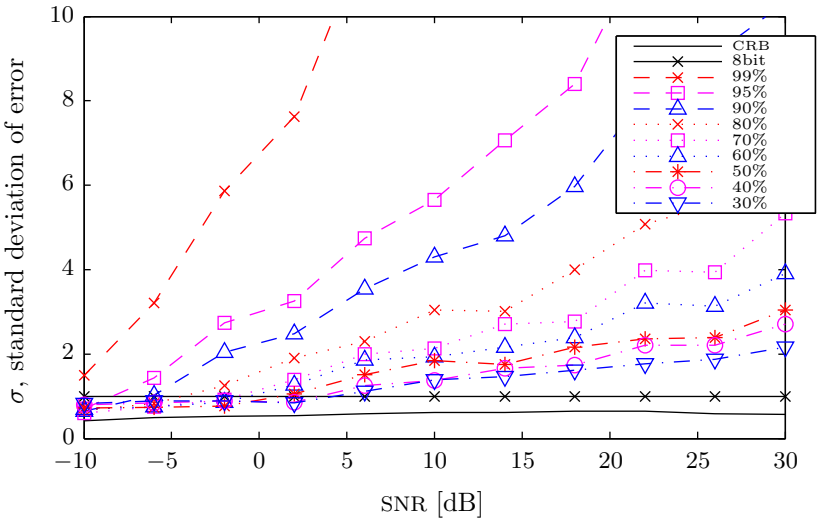

Figure 5.24: The quotient of the standard deviation of the localization error for single side band signals and time-frequency masking. The figure uses 8 bit as reference. The percentages corresponds to the amount of energy thrown. If the y axis value is 2, the σ is two times that of the 8 bit signal.

6 Recorded field data for evaluation

6.1 Introduction

To try to validate the simulations a field experiment was performed. Data was collected using four receiver positions and one transmitter position. The geometry was chosen to be similar to the one used in the simulations. However, the distance between transmitter and receiver was 5 km due to time and resource constraints. The geometry is illustrated in figure 6.1.

The forth position was not part of the original simulation array, this one was used for redundancy if some part of the field experiment failed. This was not necessary and to ensure comparability the signals recorded at this position was not used.

Due to lack of equipment only two receivers was used. One was moved between three locations, the second receiver was stationary at the forth position. The transmitter and receivers were synchronized using a time reference from Global Positioning System (GPS), so that the localization system will perceive the recordings as simultaneous.

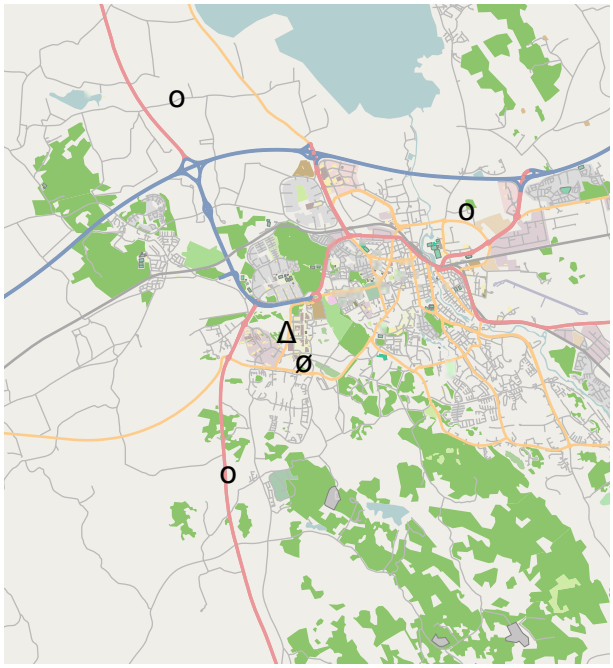

Figure 6.1: Map illustrating the transmitter position (Δ), the receiver positions (o), and the stationary receiver (ø). The location is Linköping, Sweden. The map is acquired from www.openstreetmap.org.

6.2 Signals Used

The signals used was 8-PSK, SSB, and WGN at both 2 kHz and 10 kHz bandwidth. Each signal was generated at 4 different energy levels separated by 10 dB, for a total of 24 signals. The different energy levels was combined by mod-

Signal	SNR	Frequency
FSS	20 dB	305.978 MHz
FSS	10 dB	305.982 MHz
FSS	0 dB	305.986 MHz
FSS	-10 dB	305.990 MHz
SSB	20 dB	305.994 MHz
SSB	10 dB	305.998 MHz
SSB	0 dB	306.002 MHz
SSB	-10 dB	306.006 MHz
8-PSK	20 dB	306.010 MHz
8-PSK	10 dB	306.014 MHz
8-PSK	0 dB	306.018 MHz
8-PSK	-10 dB	306.022 MHz

(a) 2 kHz signals.

Signal	SNR	Frequency
FSS	20 dB	305.890 MHz
FSS	10 dB	305.910 MHz
FSS	0 dB	305.930 MHz
FSS	-10 dB	305.950 MHz
SSB	20 dB	306.050 MHz
SSB	10 dB	306.070 MHz
SSB	0 dB	306.090 MHz
SSB	-10 dB	306.110 MHz
8-PSK	20 dB	305.970 MHz
8-PSK	10 dB	305.990 MHz
8-PSK	0 dB	306.010 MHz
8-PSK	-10 dB	306.030 MHz

(b) 10 kHz signals.

Table 6.1: Center frequencies used for each transmitted signal. SNR levels are desired levels at the mobile receiver.

ulating each signal to different frequencies. These frequencies can be found in table 6.1. The 10 kHz and 2 kHz signals was sent sequentially since they use the same frequency band. The bandwidth of the combined signals were 50 kHz and 250 kHz, respectively. The frequency spectrum of the signals, in baseband, can be found in figure 6.2 on the facing page.

6.3 Transmitting and Receiving

When receiving the signal the transmitter power was adjusted so that the received SNR at the mobile receiver was approximately 20 dB for the highest energy level signal. However, the transmitting power was limited to 5 W, some of the data recordings therefore had a lower SNR. The SNR at the stationary receiver was approximately 30 dB for the highest energy level signals.

At each position 24 recordings were performed for the 10 kHz signals and 5 recordings for the 2 kHz signals. The 10 kHz signals had a duration of 15.9 seconds, and the 2 kHz signals had a duration of 79.5 seconds. The signal length is chosen by the signal generator; it only supports signals smaller than 4 million samples. Given the total bandwidths of the signals sent, this introduces a limit of 16 and 80 seconds, respectively. A period of silence was introduced as a start-of-signal indicator.

The transmitter repetitively transmitted the signal, always starting at integer seconds using the GPS time reference. Recording was done for a period of 34.0 and 162.0 seconds respectively. This was done to assure that a complete signal would be received.

Four dipole antennas were used, each one connected to separate tuner channels on the receiver side. A computer with a data acquisition card was used to record the received signals. The tuner shifted the signals center frequency to an intermediate frequency of 10.4 MHz. This intermediate channel was connected to the data acquisition card and sampled at 160 MHz. The sampling card demodulated and decimated the signal to a sampling frequency of 156.250 kHz and 312.500 kHz for the 2 kHz and 10 kHz bandwidth signals respectively, thus fulfilling the Nyquist–Shannon sampling theorem.

The frequency spectrum for the demodulated received signals can be found in figure 6.3 on page 75. A peak is introduced around 0 kHz for the 2 kHz

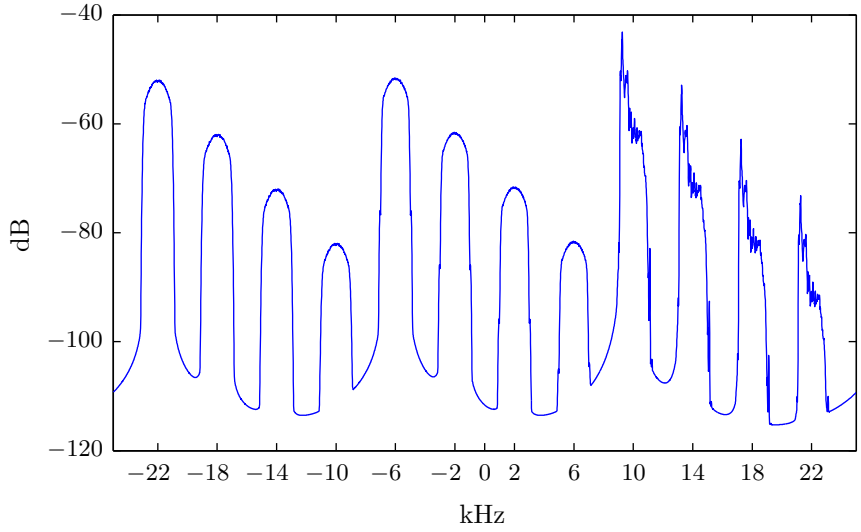

(a) Frequency spectrum for 2 kHz signals sent.

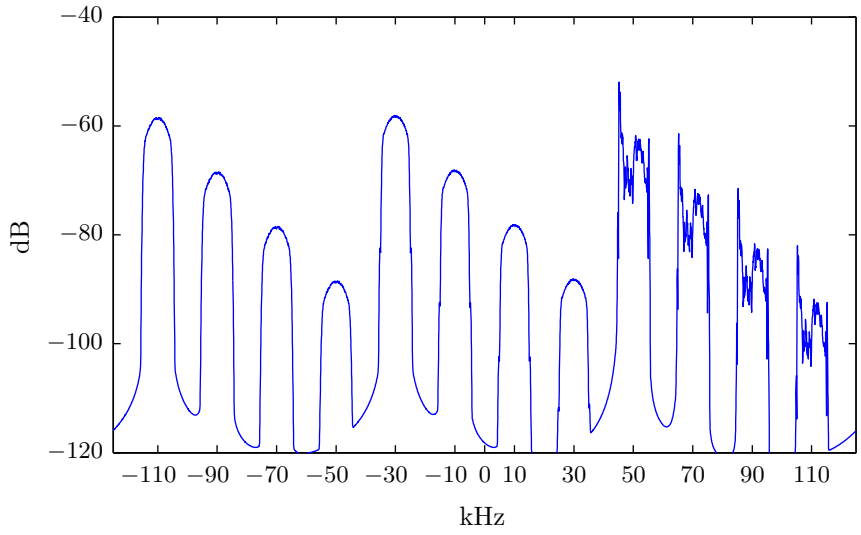

(b) Frequency spectrum for 10 kHz signals sent.

Figure 6.2: Frequency spectra for sent signals. The first four signals from left are FSS at different energy levels, the next four are PSK and the last four are SSB. The frequency values are relative to the center frequency of 306 MHz.

signals and more peaks are introduced for the 10 kHz signals. Little time was spent on figuring out why these peaks occurred since they are positioned between the signal bands and can be handled at the post processing discussed in the section below. However, one theory for the 0 kHz peak is that it is introduced because of drifting in the local oscillator in the tuner.

The peaks at approximately -20 and 24 kHz are believed to be other signals. Other concurrent measurements of the same frequency spectrum done by other Swedish Defence Research Agency (FOI) projects indicates that there were other signals present. If such signals were to be present in some of the signal bands, they would likely not correlate between recordings and have little impact on uncompressed localization ability.

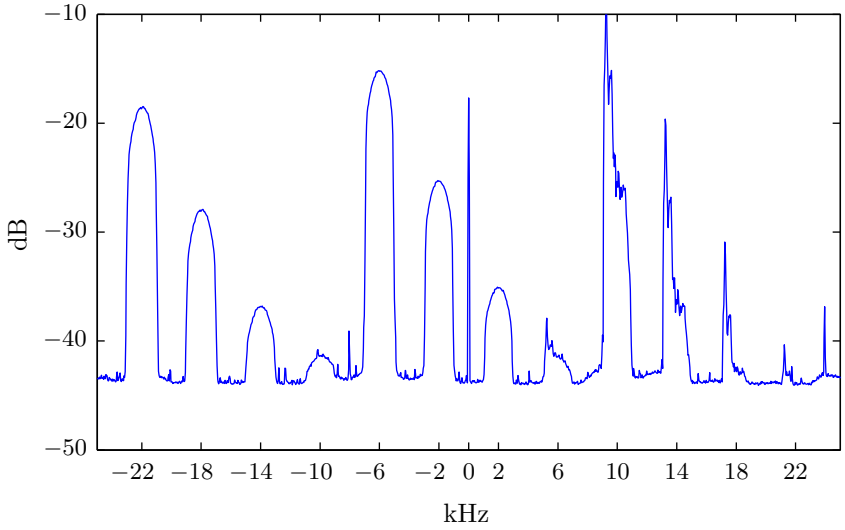

(a) Frequency spectrum for the received 2 kHz signals.

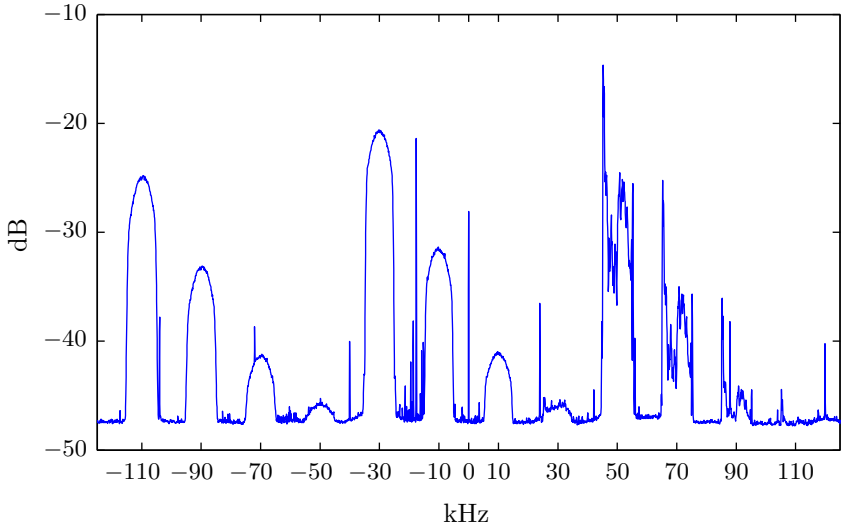

(b) Frequency spectrum for the received 10 kHz signals.

Figure 6.3: Example of frequency spectra for the received signals. The first four signals from left are FSS at different energy levels, the next four are PSK and the last four are SSB.

6.4 Post Processing

The signals were processed in MATLAB to cut out the correct parts of the signals. The transmitting and recording always started and ended at integer seconds using the GPS reference. Since each signal sampled was twice the length of the original signal sent there were silent periods in the received signals. These silent parts were used to find where the signal started and ended. The cuts were placed at integer seconds to ensure that no time delay affecting TDOA was introduced in the processing.

The signals were then demodulated and low-pass filtered to cut out the 3 different signals at the 4 different energy levels. The peaks discussed in section 6.3 on page 72 were removed by the low-pass filters. Given that four channels were used and 24 recordings were done for the 10 kHz signal a total number of 96 signals were extracted for each position, signal type and SNR level. Using the same calculation for the 2 kHz signals a total number of 20 signals were gathered for each position, signal type and SNR level.

However, for the 10 kHz bandwidth signals, one channel at each position had a SNR below 10 dB for the highest energy flat spectrum signal, these channels were discarded. A total number of 72 useful signals were therefore gathered with 10 kHz bandwidth. For the 2 kHz signals one channel was bad at two of the positions and at one of the positions the SNR was over 30 dB for one of the channels. The data from these channels where also discarded to get matching SNR levels. A total number of 15 useful signals were therefore gathered with 2 kHz bandwidth.

SNR levels were calculated using an empty frequency band between the modulated signals as noise reference. This noise band was chosen between the two flat spectrum signal with the highest energy where no peak was detected.

6.5 Localization Using Recorded Data

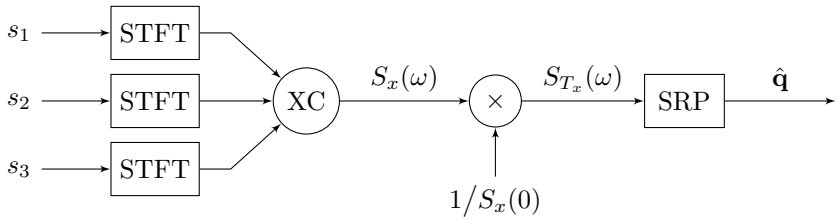

Figure 6.4: Modified localization system estimating the position from phase shift compensated cross correlation on recorded data.

The localization system used for simulation used an impulse response to filter the signal and added white Gaussian noise. A modified system was used for the field data. Since the signals have passed the actual channel no impulse response was used and no noise was added. The geometry was different so a modified grid was used to calculate the steered response power. The original grid was translated and scaled to fit the new geometry.

The output of the localization system was not as expected, the localization bias was heavy. The output, using the high SNR 10 kHz bandwidth flat spectrum signals, can be found in figure 6.5a on page 78. The bad localization performance was found to be due to that the local oscillators in the receivers was not locked in phase to each other between the recordings. This introduced a phase shift in the cross spectral density in 2.10 on page 16 which now has to

be modified to

$$S_{m\,n}(\omega) = S_s(\omega)e^{j\omega\Delta_{m,n}(\mathbf{q})}e^{j(\theta_m-\theta_n)} + S_{\nu_m\,\nu_n}(\omega), \tag{6.1}$$

where $e^{j(\theta_m-\theta_n)}$ is the result of the unlocked phases. Under ideal conditions with no noise the cross-correlation simplifies to

$$S_{m\,n}(\omega) = S_s(\omega)e^{j\omega\Delta_{m,n}(\mathbf{q})}e^{j(\theta_m-\theta_n)}. \tag{6.2}$$

By inserting $\omega_k = 0$ the expression becomes

$$S_{m\,n}(0) = S_s(0)e^{j(\theta_m-\theta_n)}. \tag{6.3}$$

It is now possible to compensate for the phase shift by dividing the cross-correlation function with $S_{m\,n}(0)$, the new compensated auto-correlation function then becomes

$$S_{T_{m\,n}}(\omega_k) = \frac{S_{m\,n}(\omega_k)}{S_{m\,n}(0)} = \frac{S_s(\omega)e^{j\omega\Delta_{m,n}(\mathbf{q})}}{S_s(0)}. \tag{6.4}$$

By doing this the localization performance was significantly increased.

This phase compensation is only possible for signals with high SNR since it assumes that there is an ideal noise free channel at $S_s(0)$. Because of this the phase shift was estimated using the high SNR signals from each measurement and applied on all the lower energy signals as well. This is not possible in real scenarios when localization is done on low SNR signals; there exists other methods to mitigate this but they are outside the scope of this thesis. The new modified localization system using phase error compensation is found in figure 6.4 on the preceding page.

The output of the modified localization system with phase shift compensation, using the same set of signals as earlier, can be found in figure 6.5b on the following page.

When using the system on the 2 kHz signals the localization result was poor. This can be seen in figure 6.6 on the next page. This can be explained by the CRB, the variance for the 2 kHz signals becomes 25 times larger given the geometry, SNR and the length of the signals used. The same poor results was achieved using the SSB speech signal with both 2 and 10 kHz bandwidth, however this is not as easy to explain and little time was spent on doing so. The PSK behaved similar to FSS.

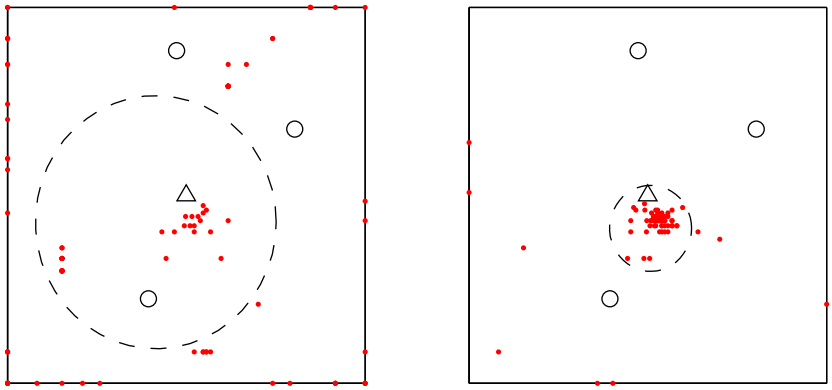

(a) Output of localization system without compensation for phase error

(b) Output of localization system with compensation for phase error

Figure 6.5: Output of localization system before and after phase error compensation for high SNR 10 kHz bandwidth FSS. The receivers are illustrated with small circles, the transmitter as a triangle and the large dashed circle has its center in the bias and its radius is the standard deviation. Each dot corresponds to an estimated position.

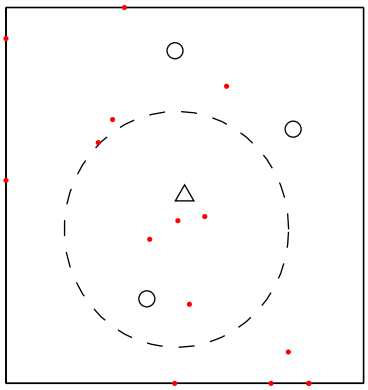

Figure 6.6: The localization output using 2 kHz bandwidth high SNR FSS. The receivers are illustrated with small circles, the transmitter as a triangle and the large dashed circle has its center in the bias and its radius is the standard deviation. Each dot corresponds to an estimated position.

6.6 Evaluation of Compression Impact

This section will only look at the effect of compression when localizing 10 kHz flat spectrum signals due to the similar behavior using PSK and poor localization results using the recorded SSB data. The presentation is to be regarded as a complement to chapter 5 on page 45.

The mean error e is calculated using the norm of the localization error along the x and y axis,

$$e = \sqrt{\mu_x^2 + \mu_y^2}. \tag{6.5}$$

The standard deviation of the error, ς, is calculated by taking the square root of the mean variance along the x and y axis.

$$\varsigma = \sqrt{\frac{\sigma_x^2 + \sigma_y^2}{2}}. \tag{6.6}$$

The localization performance for the uncompressed flat spectrum signals is found in table 6.2.

SNR	Uncompressed
−10 dB	4548
0 dB	2546
10 dB	1982
20 dB	1664

(a) Standard deviation of error

SNR	Uncompressed
−10 dB	1027
0 dB	2003
10 dB	1394
20 dB	1286

(b) Mean error

Table 6.2: Tables of the standard deviation and mean of localization error using uncompressed flat spectrum signals.

6.6.1 Compression Using DFT Components

The output of integral component quantization using DFT on the high SNR flat spectrum signals is found in figure 6.7 on the following page. The localization performance was fairly good when using 32 and 16 components compared to the uncompressed version found in figure 6.5b on the preceding page. Table 6.3 shows the standard deviation and mean of the localization error. Table 6.4 on page 81 shows the calculated ratios, all adjusted ratios is well below 1.

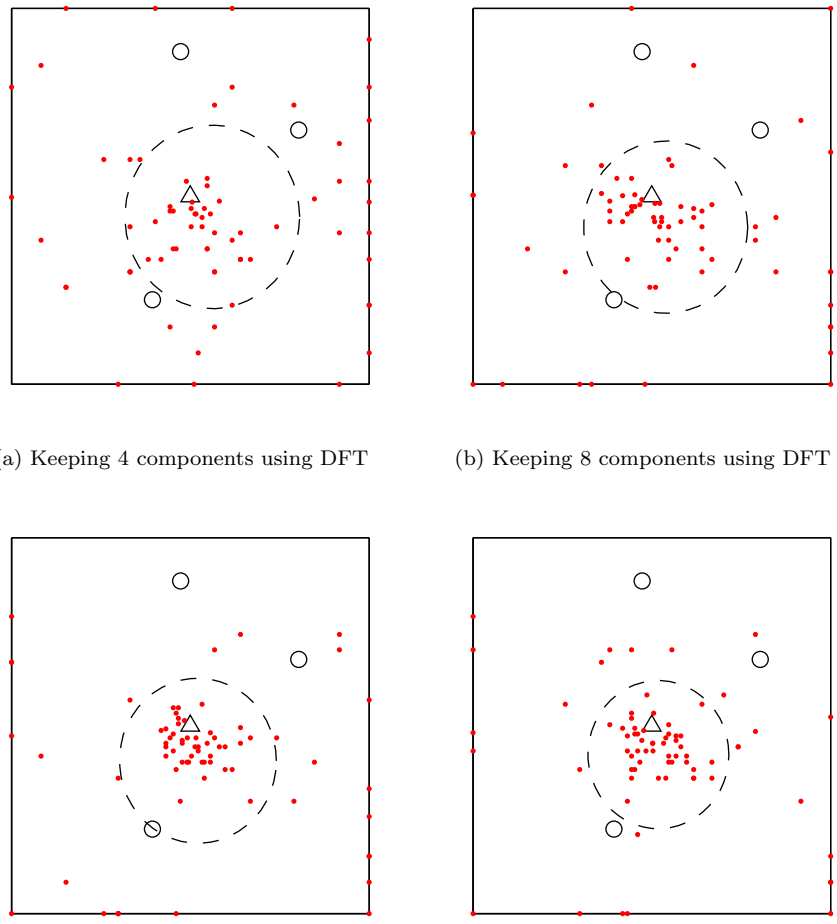

(a) Keeping 4 components using DFT

(b) Keeping 8 components using DFT

(c) Keeping 16 components using DFT

(d) Keeping 32 components using DFT

Figure 6.7: Illustrating output of localization using compression scheme with integral component quantization and DFT on high SNR flat spectrum signals. The receivers are illustrated with small circles, the transmitter as a triangle and the large dashed circle has its center in the bias and its radius is the standard deviation. Each dot corresponds to an estimated position.

SNR	$K = 1$	$K = 2$	$K = 4$	$K = 8$	$K = 16$	$K = 32$
−10 dB	2487	3285	4004	4691	4850	5279
0 dB	2562	3508	3800	4550	4480	4506
10 dB	3669	4322	3876	3463	3096	3024
20 dB	3499	3551	3550	3333	3191	2865

(a) Standard deviation of error

SNR	$K = 1$	$K = 2$	$K = 4$	$K = 8$	$K = 16$	$K = 32$
−10 dB	5701	5415	5257	3016	1040	1109
0 dB	5521	4007	2721	1150	2650	2568
10 dB	3812	1364	2215	2822	3163	3141
20 dB	2784	1346	1201	1327	1400	1160

(b) Mean error

Table 6.3: Tables of the standard deviation and mean of localization error using integral component quantization with DFT on flat spectrum signals.

SNR	$K = 1$	$K = 2$	$K = 4$	$K = 8$	$K = 16$	$K = 32$
−10 dB	0.00	0.01	0.02	0.03	0.06	0.12
0 dB	0.00	0.01	0.02	0.03	0.06	0.12
10 dB	0.00	0.01	0.02	0.03	0.06	0.12
20 dB	0.00	0.01	0.02	0.03	0.06	0.12

(a) Ratio.

SNR	$K = 1$	$K = 2$	$K = 4$	$K = 8$	$K = 16$	$K = 32$
−10 dB	0.00	0.00	0.01	0.03	0.07	0.17
0 dB	0.00	0.01	0.03	0.10	0.19	0.39
10 dB	0.01	0.03	0.06	0.09	0.15	0.29
20 dB	0.02	0.03	0.07	0.12	0.23	0.37

(b) Adjusted ratio.

Table 6.4: Ratio calculations using integral component quantization with DFT on flat spectrum signals.

6.6.2 Compression Using KLT Components

The output of integral quantization using KLT on the high SNR flat spectrum signals is found in figure 6.8 on the next page. The localization performance was fairly good when using 32, 16 and 8 components compared to the uncompressed version found in figure 6.5b on page 78. Table 6.5 on page 83 show the standard deviation and mean of the localization error. Table 6.6 on page 83 shows the calculated ratios, all adjusted ratios is well below 1.

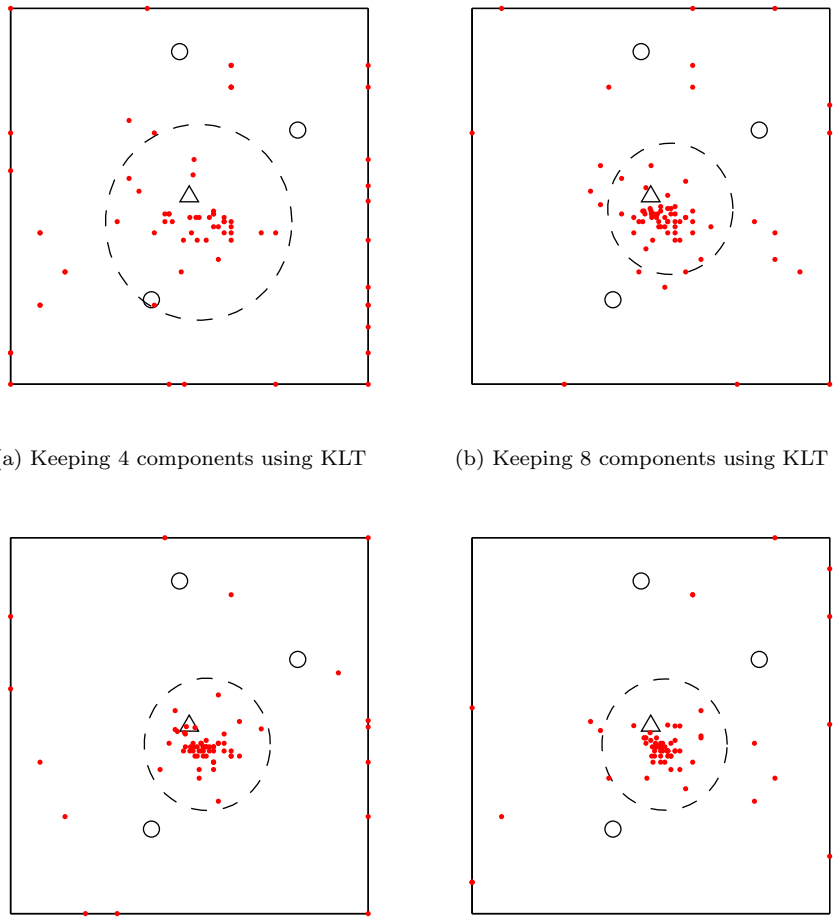

(a) Keeping 4 components using KLT

(b) Keeping 8 components using KLT

(c) Keeping 16 components using KLT

(d) Keeping 32 components using KLT

Figure 6.8: Illustrating output of localization using compression scheme with integral component quantization and KLT on high SNR flat spectrum signals. The receivers are illustrated with small circles, the transmitter as a triangle and the large dashed circle has its center in the bias and its radius is the standard deviation. Each dot corresponds to an estimated position.

SNR	$K = 1$	$K = 2$	$K = 4$	$K = 8$	$K = 16$	$K = 32$
−10 dB	5177	5427	5245	5082	5067	5170
0 dB	5371	5186	5304	5112	4438	4101
10 dB	5469	4599	4502	3107	2851	2755
20 dB	5121	4231	3789	2542	2563	2543

(a) Standard deviation of error

SNR	$K = 1$	$K = 2$	$K = 4$	$K = 8$	$K = 16$	$K = 32$
−10 dB	818	668	770	435	396	924
0 dB	716	1660	1444	439	701	1488
10 dB	522	449	1110	2202	1625	1325
20 dB	731	401	1082	937	1035	927

(b) Mean error

Table 6.5: Tables of the standard deviation and mean of localization error using integral component quantization with KLT on flat spectrum signals.

SNR	$K = 1$	$K = 2$	$K = 4$	$K = 8$	$K = 16$	$K = 32$
−10 dB	0.01	0.01	0.03	0.06	0.11	0.23
0 dB	0.01	0.01	0.03	0.06	0.11	0.23
10 dB	0.01	0.01	0.03	0.06	0.11	0.23
20 dB	0.01	0.01	0.03	0.06	0.11	0.23

(a) Ratio.

SNR	$K = 1$	$K = 2$	$K = 4$	$K = 8$	$K = 16$	$K = 32$
−10 dB	0.01	0.02	0.03	0.06	0.13	0.26
0 dB	0.02	0.04	0.08	0.15	0.24	0.43
10 dB	0.03	0.05	0.09	0.10	0.18	0.34
20 dB	0.04	0.06	0.09	0.10	0.20	0.39

(b) Adjusted ratio.

Table 6.6: Ratio calculations using integral component quantization with KLT on flat spectrum signals.

6.6.3 Compression Using Partial Components

The partial components worked good down to 2 bits on average per component. The localization output for the high SNR flat spectrum signals can be found in figure 6.9 on the next page, for comparison the uncompressed version is found in 6.5b on page 78. Table 6.7 on page 85 shows the standard deviation and mean of the localization error. Table 6.8 on page 85 shows the calculated ratios, the localization performance adjusted ratios is slightly lower than the original ratios.

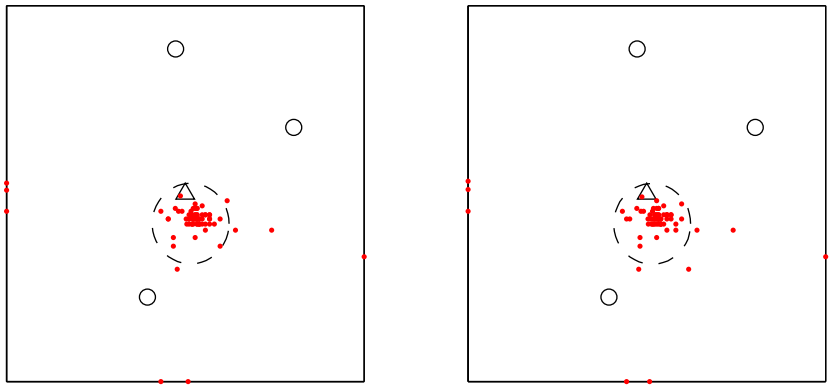

(a) Assigning 6 bits using partial components (b) Assigning 4 bits using partial components

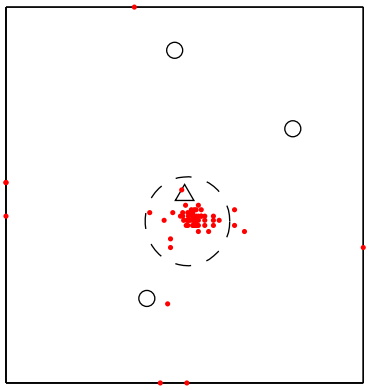

(c) Assigning 2 bits using partial components

Figure 6.9: Illustrating output of localization using compression scheme with partial component quantization and DFT. The receivers are illustrated with small circles, the transmitter as a triangle and the large dashed circle has its center in the bias and its radius is the standard deviation. Each dot corresponds to an estimated position.

SNR	2 bits	4 bits	6 bits
−10 dB	4538	4455	4478
0 dB	2741	2753	2592
10 dB	1842	1800	1797
20 dB	1720	1564	1559

(a) Standard deviation of error

SNR	2 bits	4 bits	6 bits
−10 dB	1028	753	740
0 dB	2316	2196	2097
10 dB	1301	945	1039
20 dB	1026	1195	1185

(b) Mean error

Table 6.7: Tables of the standard deviation and mean of localization error using partial component quantization with DFT.

SNR	2 bits	4 bits	6 bits
−10 dB	0.50	1.00	1.50
0 dB	0.50	1.00	1.50
10 dB	0.50	1.00	1.50
20 dB	0.50	1.00	1.50

(a) Ratio.

SNR	2 bits	4 bits	6 bits
−10 dB	0.50	0.96	1.45
0 dB	0.58	1.17	1.56
10 dB	0.43	0.82	1.23
20 dB	0.53	0.88	1.32

(b) Adjusted ratio.

Table 6.8: Ratio calculations using partial component quantization with DFT on flat spectrum signals.

6.6.4 Compression Using Time-Frequency Masking

For time-frequency masking, “70%” should be interpreted as “70% of the energy is cut”. The compression behaves well when cutting smaller amounts of data, this is consistent with the simulations. For the high SNR signal the output is illustrated in figure 6.10 to 6.11 on pages 86–87. Table 6.9 on page 88 shows the standard deviation and mean of the localization error. The standard deviation is significantly less when cutting 30% than cutting 99% for the high SNR signals. Table 6.10 on page 88 shows the calculated ratios, almost all adjusted ratios are below 1.

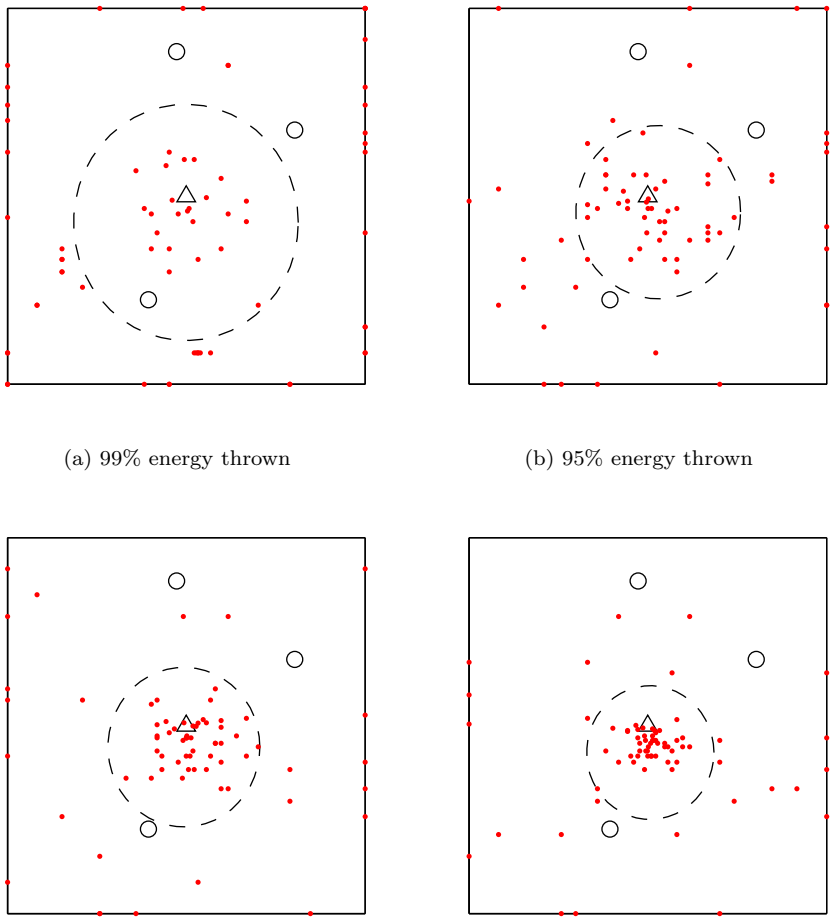

(a) 99% energy thrown

(b) 95% energy thrown

(c) 90% energy thrown

(d) 80% energy thrown

Figure 6.10: Illustrating output of localization using compression scheme with time-frequency masking for high SNR flat spectrum signals. The receivers are illustrated with small circles, the transmitter as a triangle and the large dashed circle has its center in the bias and its radius is the standard deviation. Each dot corresponds to an estimated position.

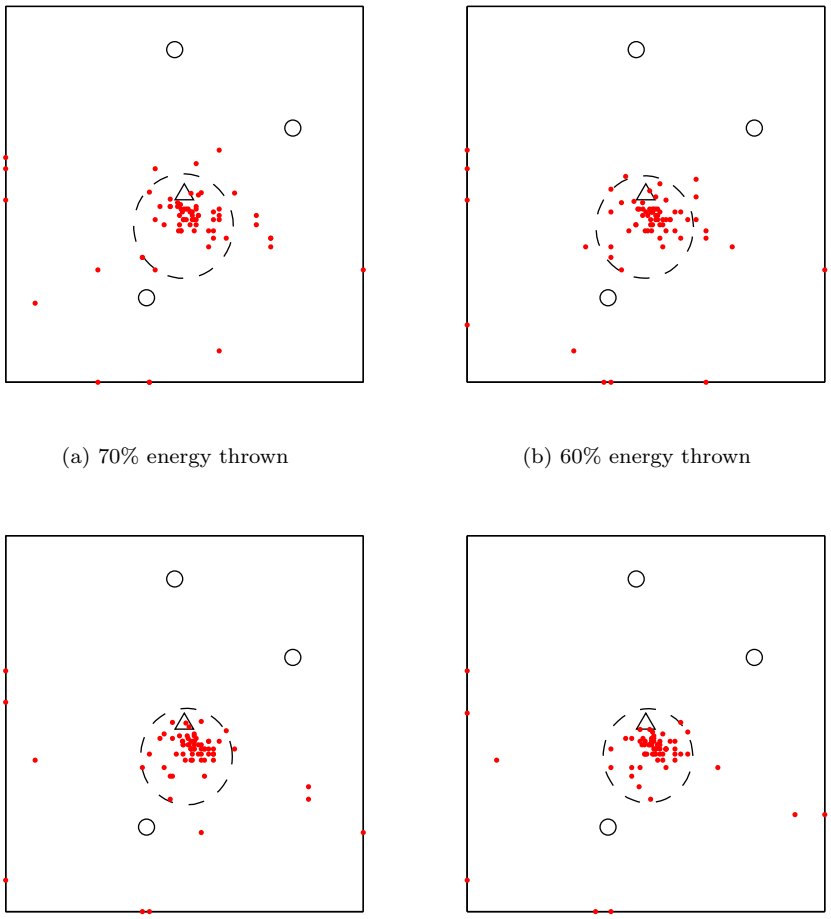

(a) 70% energy thrown

(b) 60% energy thrown

(c) 40% energy thrown

(d) 30% energy thrown

Figure 6.11: Illustrating output of localization using compression scheme with time-frequency masking on high SNR flat spectrum signals. The receivers are illustrated with small circles, the transmitter as a triangle and the large dashed circle has its center in the bias and its radius is the standard deviation. Each dot corresponds to an estimated position.

SNR	30%	40%	60%	70%	80%	90%	95%	99%
−10 dB	4799	4679	4683	5013	5008	5045	5296	4926
0 dB	2946	3058	3393	4123	4431	4960	5405	4713
10 dB	2092	2169	2522	2665	3109	3608	4176	5034
20 dB	1820	1866	1979	2023	2585	3087	3349	4569

(a) Standard deviation of error

SNR	30%	40%	60%	70%	80%	90%	95%	99%
−10 dB	553	489	1053	1423	1107	1447	1122	1539
0 dB	2043	2294	2350	1751	1540	1635	710	1326
10 dB	1469	1509	1520	1440	1060	1349	1384	707
20 dB	1252	1283	1270	1235	1052	839	753	1016

(b) Mean error

Table 6.9: Tables of the standard deviation and mean of localization error using time-frequency masking on flat spectrum signals.

SNR	30%	40%	60%	70%	80%	90%	95%	99%
−10 dB	0.76	0.60	0.37	0.28	0.21	0.16	0.14	0.13
0 dB	0.75	0.59	0.36	0.28	0.21	0.16	0.14	0.13
10 dB	0.73	0.57	0.35	0.27	0.21	0.16	0.14	0.13
20 dB	0.70	0.55	0.34	0.27	0.20	0.16	0.14	0.13

(a) Ratio.

SNR	30%	40%	60%	70%	80%	90%	95%	99%
−10 dB	0.85	0.64	0.39	0.34	0.26	0.19	0.19	0.15
0 dB	1.01	0.86	0.65	0.73	0.64	0.60	0.62	0.44
10 dB	0.81	0.68	0.57	0.49	0.51	0.52	0.61	0.82
20 dB	0.84	0.70	0.48	0.39	0.49	0.54	0.56	0.96

(b) Adjusted ratio.

Table 6.10: Ratio calculations using time-frequency masking on flat spectrum signals.

7 Conclusion and discussion

7.1 Comments on Compression and Noise

There are several aspects of noise needed to be considered when applying data compression in a TDOA system. This section will discuss a few of them.

7.1.1 Separate Signal from Noise

As mentioned in section 3.2 on page 23, different signals pose different difficulties when separating them from the noise. For weak (low SNR) noise-like signals, such as FSS with white Gaussian noise, it is hard to distinguish relevant signal information from noise in a single receiver. However, as the signal length increases, cross correlation will be able to find the signal anyway since the noise is assumed to be uncorrelated; TDOA works for negative SNR Falk (2004). This means that information that is impossible, or at least very hard, to label as important in a single node might be useful in the correlation system.

7.1.2 Noise Reduction

For radar signals, it has been shown that a compression ratio of about 1:100 can be achieved using Singular Value Decomposition (SVD) with little impact on TDOA localization Fowler *et al.*. This is in part because compression can actually increase the SNR, since transform components with more energy often contains a higher percentage of signal information than the components with less energy do. This is why some of the compression schemes used performs better at lower SNR levels in terms of adjusted ratio. This denoising effect is seen in figure 4.15 on page 44. All curves show the same trend at low SNR but those with lower data rate performes worse at high SNR. Thus, the performance adjusted ratio will be worse for high SNR signals at low data rates.

7.2 Comments on the Field Recordings

The behavior of the compressed flat spectrum signals from the recorded field data was similar to the ones used in the simulations. This supports the theory that compression can be applied in actual TDOA localization systems.

When using the single side band signals together with the localization system the output was not as expected. Why this is so was not thoroughly investigated. This neither prove or disprove the results of the simulations, further studies are needed.

The drifting in the local oscillator mentioned in section 6.3 on page 72 could be of significance, especially when localization is done on narrow bandwidth signals. While studying the frequency spectrum of the received signal, using a high number of frequency bins, the drift was estimated to be approximately 2 Hz. When estimating the TDOA 512 frequency bins was used, this gives approximately 4 Hz width of each bin for the 2 kHz signal. By decreasing the number of frequency bins the impact of drifting could be reduced. Another method could be using a automatic frequency control circuit in the tuner.

The adjusted ratios was good when using the compression schemes on the recorded data, the compression had little impact on the standard deviation of the localization error. However, the adjusted ratios and standard deviations

calculated using the recorded data has low precision due to the granularity in the steered response power grid. This will have to be considered when interpreting the data. When simulating, the estimated positions were gathered at the dense part of the grid. Since the error were higher for the recorded data the precision was reduced. A more fine grained grid would shine some more light on the localization precision.

7.3 Proposed Use

Data compression in a localization system is a non-trivial problem, but not a useless one. In the introduction chapter (page 11), the motivation behind it was presented. This thesis work has not found a good catch-all compression scheme, but shines some light on possible solutions if the sought after signal is of a known type. The compression scheme using partial components gives interesting results, the signal independent trend of the 2 bits partial component adjusted ratio values is promising. This compression scheme should be fine tuned before actual use, but seems to be able to successfully compress the data. A combination of partial components and time-frequency masking could improve the result. For SSB signals, several of the tested compression schemes gave good results.

7.4 Localization Ability Reduction

If lower localization accuracy is tolerated, compression can do more. A lot of the adjusted compression ratio numbers presented in chapter 5 are well above 1 due to compensation for reduced accuracy. In general, there is a trade off between data rate and localization ability, see section 4.4 on page 42.

7.5 Future

This section discusses areas where further research can be done.

7.5.1 Amplitude Data

It may be possible to cut the data needed to be transmitted from all but one node in half by simply discarding the magnitude data and only keeping the phase data, and estimating the amplitude from the one node that did not discard its amplitude data. This is more convenient if one of the nodes is part of the system which does the correlation and localization; this is often the case. Using one of the listening nodes as base node would also partly solve the component selection problem presented in section 4.2.1.1 on page 34, one less signal need to be compressed.

7.5.2 Phase-amplitude Data Optimization

Further effort should be spent on combining bit allocation schemes with an amplitude-phase data consideration and combine this with a TFM scheme. Most of the TDOA relevant information exists in the phase data when the receivers are less than a wave length away from the transmitter. Allocating schemes that takes this into consideration could improve the results. An optimization problem approach to the trade off between amplitude and phase data might be a useful way forward.

7.5.3 Block Length and Ratio

The block length chosen has an impact on the compression results, both in quality and ratio. Exactly how depends on compression scheme and signal type, and to what end the data is used for. For noise-like signals, the DFT block length should be more thoroughly studied, one idea is that there are signal type dependent optimal block lengths.

7.5.4 Impact on Node-Base Transmission Redundancy

Like in most compression schemes, redundancy between data points is reduced. If the transmission between a system node (that uses compression) and the node responsible for the correlation introduces bit errors, the results may be worse off than it would have been without compression. However, the compression schemes use block overlap and introduce redundancy to the transmitted signals.

These effects, and whether there will be graceful degradation[1] or not, are out of scope.

7.5.5 Other Areas to Look at

It would be interesting to investigate adaptive compression schemes, to see if systems that use higher order cumulants and moments to fit signal to known distribution types can achieve better compression rates.

Looking into the signals received, e.g. phase shift in constellation points for PSK, might give *very* good compression rates for high SNR levels.

[1] *"Graceful degradation: Degradation of a system in such a manner that it continues to operate, but provides a reduced level of service rather than failing completely,"* ATIS (2001)

Lists

List of Figures

List of Tables

List of Algorithms

Bibliography

Algazi, V. R. & Sakrison, D. J. 1969 On the optimality of the Karhunen-Loéve expansion (corresp.). *Information Theory, IEEE Transactions on*, **15**(2), 319 – 321. ISSN 0018-9448.

Andersson, B., Bergdal, H., Gustavsson, R., Nagy, P. & Oscarsson, F. 2004a Signalspaningsteknik del 1 – Grunder samt radiosignalspaning. Kompendium, Institutionen för Telekrigsystem, FOI, Linköping. Sammanställt av Hans Bergdal.

Andersson, B., Bergdal, H. & Lindgren, B. 2004b Signalspaningsteknik del 2 – Radarsignalspaning. Kompendium, Institutionen för Telekrigsystem, FOI, Linköping. Sammanställt av Hans Bergdal.

ATIS 2001 ANS T1.523-2001, Telecom Glossary 2000.
URL: `http://www.atis.org/glossary/`.

Carlson, A. B. 2002 *Communication systems: an introduction to signals and noise in electrical communication*. McGraw-Hill New York,, 4th ed. edition. ISBN 0-07-112175-7. ISBN 0-07-112175-7.

Cook, G. J. 2003 *Shaped Response Interpolation: Direction of Arrival Estimation with Microphone Arrays in Reverberant Environments*. Master thesis, Curtin University of Technology.

Cover, T. M. & Thomas, J. A. 2006 *Elements of Information Theory 2nd Edition*. Wiley Series in Telecommunications and Signal Processing. Wiley-Interscience, 2 edition. ISBN 0471241954. ISBN 0-471-24195-4.

Dmochowski, J., Benesty, J. & Affes, S. 2007 A generalized steered response power method for computationally viable source localization. *Audio, Speech, and Language Processing, IEEE Transactions on*, **15**(8), 2510 –2526. ISSN 1558-7916. doi:10.1109/TASL.2007.906694.

Falk, J. 2004 *An electronic warfare perspective on time difference of arrival estimation subject to radio receiver...* Master thesis, Kungliga Tekniska Högskolan, Stockholm. Lic.-avh. Stockholm : Tekn. högsk., 2004.

Fowler, M. L. 1999 Data compression for TDOA/DD location system. Patent. US 5,991,454.

Fowler, M. L., Chen, M. & Binghamton, S. 2005 Fisher-information-based data compression for estimation using two sensors. *Aerospace and Electronic Systems, IEEE Transactions on*, **41**(3), 1131 – 1137. ISSN 0018-9251. doi: 10.1109/TAES.2005.1541459.

Fowler, M. L., Chen, M., Johnson, J. A. & Zhou, Z. ???? Data compression using SVD and Fisher information for radar emitter location. URL: `http://www.ws.binghamton.edu/fowler`.

Hotelling, H. 1933 Analysis of a complex of statistical variables into principal components. *Journal of Educational Psychology*, **24**(6-7), 498–520. ISSN 0022-0663.

Jayant, N. & Noll, P. 1984 *Digital Coding of Waveforms*. Ignatius Press, San Francisco. ISBN 0132119137. ISBN 0132119137.

Johansson, A. 2008a *Acoustic Sound Source Localisation and Tracking – in Indoor Environments*. Dissertation, Blekinge Institute of Technology. ISBN 978-91-7295-133-4.

Johansson, A. 2008b Pejltekniker i ett taktiskt KOS system. Memo, Institutionen för Telekrigsystem, FOI, Linköping. FOI Memo 2581.

Knapp, C. & Carter, G. 1976 The generalized correlation method for estimation of time delay. *Acoustics, Speech and Signal Processing, IEEE Transactions on*, **24**(4), 320–327. ISSN 0096-3518.

Pursley, M. B. 2002 *Random Processes in Linear Systems*. Prentice Hall. ISBN 0-13-067391-9.

Rao, K. & Yip, P. 1990 *Discrete Cosine Transform: Algorithms, Advantages, Applications*. Academic Press. ISBN 0-12-580203-X.

Sayood, K. 2005 *Introduction to Data Compression, Third Edition*. Morgan Kaufmann Publishers Inc., San Francisco, CA, USA. ISBN 012620862X.